

SISALv3: A global speleothem stable isotope and trace element database

Nikita Kaushal^{1*}, Franziska A. Lechleitner^{2*}, Micah Wilhelm³, Khalil Azennoud⁴, Janica C. Bühler⁵,
5 Kerstin Braun⁶, Yassine Ait Brahim⁴, Andy Baker⁷, Yuval Burstyn⁸, Laia Comas-Bru⁹, Jens
Fohlmeister¹⁰, Yonaton Goldsmith¹¹, Sandy P. Harrison¹², István G. Hatvani^{13,14}, Kira Rehfeld⁵,
Magdalena Ritzau⁵, Vanessa Skiba^{15, 16}, Heather M. Stoll¹⁷, József G. Szűcs¹⁸, Péter Tanos¹⁸, Pauline C.
Treble^{7,19}, Vitor Azevedo²⁰, Jonathan L. Baker^{21,22}, Andrea Borsato²³, Sakonvan Chawchai²⁴, Andrea
Columbu²⁵, Laura Endres¹⁷, Jun Hu²⁶, Zoltán Kern^{13,14}, Alena Kimbrough²⁷, Koray Koç^{28,29}, Monika
10 Markowska^{30,31}, Belen Martrat³², Syed Masood Ahmad³³, Carole Nehme³⁴, Valdir Felipe Novello⁵, Carlos
Pérez-Mejías²¹, Jiaoyang Ruan^{35,36}, Natasha Sekhon^{37,38}, Nitesh Sinha^{35,36}, Carol V. Tadros^{7,19}, Benjamin
H. Tiger^{39,40}, Sophie Warken^{41,42}, Annabel Wolf⁴³, Haiwei Zhang²¹ and SISAL Working Group members⁺

¹Exeter College, University of Oxford, Oxford OX1 3DP, UK; Now at the American Museum of Natural History, New York
15 10024, United States of America

²Department of Chemistry, Biochemistry and Pharmaceutical Sciences, and Oeschger Centre for Climate Change Research,
University of Bern, Freiestrasse 3, 3012 Bern, Switzerland

³Swiss Federal Institute for Forest, Snow and Landscape Research WSL, Zürcherstrasse 111, 8903 Birmensdorf, Switzerland

⁴International Water Research Institute, Mohammed VI Polytechnic University, Lot 660 Hay Moulay Rachid, 43150,
20 Benguerir, Morocco

⁵Department of Geoscience and Department of Physics, Geo- und Umweltforschungszentrum (GUZ), Schnarrenbergstr. 94/96,
72076 Tübingen, Germany

⁶Arizona State University, Institute of Human Origins, PO Box 878404, Tempe, AZ 85287, USA

⁷ School of Biological, Earth and Environmental Sciences, UNSW Sydney, Sydney, NSW, 2052, Australia

²⁵UC Davis Institute for the Environment, UC Davis Earth and Planetary Sciences, University of California Davis, One Shields
Avenue, Davis, CA 95616, USA

⁹Barcelona, Spain

¹⁰Federal Office for Radiation Protection, Koepenicker Allee 120, 10318 Berlin, Germany

¹¹The Fredy & Nadine Herrmann Institute of Earth Sciences, The Hebrew University, The Edmond J. Safra Campus - Givat
30 Ram, Jerusalem 9190401, Israel

¹²Department of Geography and Environmental Science, University of Reading, Reading RG6 6AH, UK

¹³ Institute for Geological and Geochemical Research, HUN-REN Research, Research Centre for Astronomy and Earth
Sciences, Budaörsi út 45, H-1112 Budapest, Hungary

¹⁴CSFK, MTA Centre of Excellence, Budapest, Konkoly Thege Miklós út 15-17, 1121 Budapest, Hungary

³⁵ Potsdam Institute for Climate Impact Research (PIK), Potsdam, Germany

¹⁶ Alfred Wegener Institute (AWI), Helmholtz Centre for Polar and Marine Research, Potsdam, Germany.

¹⁷Department of Earth Sciences, ETH Zurich, Sonneggstrasse 5, 8092 Zurich, Switzerland

¹⁸ Department of Geology, Institute of Geography and Earth Sciences, ELTE Eötvös Loránd University, Budapest, 1117,
Hungary

⁴⁰ANSTO, New Illawarra Road, Lucas Heights, NSW 2234, Australia

²⁰Department of Geology, Trinity College Dublin, Dublin 2, Ireland

²¹Institute of Global Environmental Change, Xi'an Jiaotong University, Xi'an, Shaanxi, China 710049

²²Institute of Geology, Innsbruck University, Innrain 52, Innsbruck 6020, Austria

²³School of Environmental and Life Sciences, The University of Newcastle, NSW 2308, Australia

- 45 ²⁴Department of Geology, Faculty of Science, Chulalongkorn University, Bangkok 10330 Thailand
²⁵University of Pisa, Department of Earth Sciences, Via Santa Maria 53, 56126 Pisa Italy
²⁶College of Ocean and Earth Sciences, Xiamen University, Xiamen, Fujian, 361102, China
²⁷School of Earth, Atmospheric and Life Sciences, University of Wollongong, Northfields Ave Wollongong, NSW 2522, Australia
50 ²⁸Department of Geological Engineering, Akdeniz University, 07100, Antalya, Türkiye
²⁹Quaternary Geology, Department of Environmental Sciences, University of Basel, 4056, Switzerland
³⁰Department of Climate Geochemistry, Max Planck Institute for Chemistry, Mainz, Germany
³¹Department of Geography and Environmental Sciences, Northumbria University, Newcastle upon Tyne, NE1 8ST, United Kingdom
55 ³²Department of Environmental Chemistry, Institute of Environmental Assessment and Water Research (IDAEA-CSIC), Jordi Girona, 18; 08034 Barcelona, Spain
³³Inter-University Accelerator Centre, New Delhi 110067, India
³⁴UMR IDEES 6266, CNRS, University of Rouen Normandy, 1, Rue Thomas Becket, Mont Saint-Aignan, 76130, France
60 ³⁵Center for Climate Physics, Institute for Basic Science, Busan, 46241, Republic of Korea
³⁶Pusan National University, Busan, 46241, Republic of Korea
³⁷Department of Earth, Environmental and Planetary Science, Brown University, Providence 02908, Rhode Island, USA
³⁸Institute at Brown for Environment and Society, Brown University, Providence 02908, Rhode Island, USA
³⁹Department of Earth, Atmospheric and Planetary Sciences, Massachusetts Institute of Technology, Cambridge, MA, USA
⁴⁰Department of Geology and Geophysics, Woods Hole Oceanographic Institution, Woods Hole, MA, USA
65 ⁴¹Ruprecht Karls University Heidelberg, Institute of Earth Sciences, Im Neuenheimer Feld 234, 69120 Heidelberg
⁴²Ruprecht Karls University Heidelberg, Institute of Environmental Physics, Im Neuenheimer Feld 229, 69120 Heidelberg
⁴³Department of Earth System Science, University of California Irvine, Croul Hall, Irvine, CA 92697-3100, USA
+ A full list of authors appears at the end of the paper.

70 *These authors contributed equally to the manuscript.

Correspondence to: Nikita Kaushal (nikitageologist@gmail.com), Franziska Lechleitner (Franziska.lechleitner@unibe.ch),
Micah Wilhelm (micah.wilhelm@wsl.ch)

Abstract. Paleoclimate information on multiple climate variables at different spatiotemporal scales is increasingly important to understand environmental and societal responses to climate change. A lack of high-quality reconstructions of past hydroclimate has recently been identified as a critical research gap. Speleothems, with their precise chronologies, widespread distribution, and ability to record changes in local to regional hydroclimate variability, are an ideal source of such information. Here we present a new version of the Speleothem Isotopes Synthesis and AnaLysis database (SISALv3), which has been expanded to include trace element ratios and Sr-isotopes as additional, hydroclimate-sensitive geochemical proxies. The oxygen and carbon isotope data included in previous versions of the database have been substantially expanded. SISALv3, 75 contains speleothem data from 365 sites from across the globe, including 95 Mg/Ca, 85 Sr/Ca, 52 Ba/Ca, 25 U/Ca, 29 P/Ca and 14 Sr-isotope records. The database also has increased spatiotemporal coverage for stable oxygen (892) and carbon (620) isotope records compared to SISALv2 (673 and 430 stable oxygen and carbon records, respectively). Additional meta information has been added to improve machine-readability and filtering of data. Standardized chronologies are included for all new entities together with the originally published chronologies. The SISALv3 database thus constitutes a unique resource 80 of speleothem paleoclimate information that allows regional-to-global paleoclimate analyses based on multiple geochemical

proxies, allowing more robust interpretations of past hydroclimate and comparisons with isotope-enabled climate models and other earth system and hydrological models. The database can be accessed at <http://dx.doi.org/10.5287/ora-2nanwp4rk>.

1 Introduction

Speleothems, secondary cave carbonate precipitates, are a rich paleoenvironmental archive of geochemical data (Wong and Breecker, 2015). Due to their widespread distribution (Comas-Bru et al., 2020) and their precise chronologies (Henderson, 2006), they can provide paleoclimate data at seasonal (Baldini et al., 2021) to multi-annual resolution spanning millennial and longer time scales (Cheng et al., 2016; Stoll et al., 2022).

The Speleothem Isotopes Synthesis and AnaLysis working group (SISAL WG) is an international effort to synthesize speleothem data under the umbrella of the Past Global Changes (PAGES) project (Comas-Bru et al., 2017; Comas-Bru and Harrison, 2019). The SISAL WG aims to answer critical open questions in paleoclimate science with a focus on regional to global trends and event synchronization. To address these questions, the SISAL WG has been developing standardized and quality checked databases. The first three versions of the database (SISALv1, SISALv1b and SISALv2) provided the paleoclimate community with a growing resource of speleothem geochemical data (Atsawawaranunt et al., 2018; Comas-Bru et al., 2020, 2019), specifically oxygen ($\delta^{18}\text{O}$) and carbon ($\delta^{13}\text{C}$) isotope records, and age-model ensembles, along with an online tool -the SISAL webApp - to increase accessibility to the SISAL database (Hatvani et al., 2024). The SISAL database versions have been exploited (i) to better understand the drivers of speleothem environmental proxies and improve their interpretations (Baker et al., 2019, 2021; Fohlmeister et al., 2020; Treble et al., 2022; Skiba and Fohlmeister, 2023), (ii) to provide a resource on the interpretation of speleothem records at a regional level, identifying key gaps and future work (Kaushal et al., 2018; Lechleitner et al., 2018; Braun et al., 2019a; Burstyn et al., 2019; Deininger et al., 2019; Kern et al., 2019; Oster et al., 2019; Zhang et al., 2019; Lorrey et al., 2020), and (iii) to understand the mechanisms of past climate change including through comparison with isotope-enabled climate models (Comas-Bru et al., 2019; Parker et al., 2021a; Bühler et al., 2022; Parker and Harrison, 2022; Parker et al., 2021b) and other modelling approaches (Skiba et al., 2023).

The new SISALv3 database provides an increased dataset of oxygen and carbon isotope data, interpreted as records of hydroclimate and vegetation dynamics/bioproduction (Wong and Breecker, 2015), and has been significantly expanded to include data on Sr, Mg, Ba, U, typically tracers for hydrological processes in the karst and cave (Fairchild et al., 2000; Johnson et al., 2006; Fairchild and Treble, 2009; Wassenburg et al., 2016), and P, recognized as tracer for surface bioproduction (Treble et al., 2003; Borsato et al., 2007; McDonough et al., 2022) (Table 1). Also included are data on Sr-isotopes, as these are an important proxy for hydroclimatic processes and may provide information on local hydrology and soil source, production and/or erosion (e.g., Li et al., 2005; Ünal-İmer et al., 2016; Wortham et al., 2017; Weber et al., 2018; Ward et al., 2019; Utida et al., 2020). Ratios of Sr/Ca, Mg/Ca, Ba/Ca and U/Ca, coupled with $\delta^{13}\text{C}$ information, are sensitive to water-rock interactions and residence time (Fairchild et al., 2000; Johnson et al., 2006). An important mechanism that drives variability in these multiple proxies in quantifiable ways is the process of prior calcite/carbonate precipitation (PCP), through which

carbonate precipitated along flow paths in the karst and on the cave roof will lead to altered element concentration in cave drip waters from which the speleothem ultimately precipitates (Fairchild et al., 2000; Day and Henderson, 2013). An increase in

120 PCP usually occurs in times of drought that facilitate increased water-rock residence times and degassing in the karst (Fairchild et al, 2000). The strength of these proxies is that they provide robust climatic and environmental information via a multi-proxy approach that will need to be tailored for different karst and climatic settings (Table 1). The SISAL Working Group is currently working on projects with the new additional proxies to explore and gain more detailed insights. We provide examples of proxy interpretations with linked references, but we must emphasize that this list is not exhaustive, the interpretations are time-scale 125 dependent, and in most cases, multi-proxy approaches are necessary (Table 1). The SISALv3 database, augmented with trace element proxies thus provides a multi-proxy dataset that can be used for long-term drought reconstructions in the past, and to better understand the forcings, mechanisms and periodicities of such events. In addition to the new geochemical data, extensive metadata including information on parameters such as vegetation and karst type as well as entity (i.e. speleothem dataset) images are provided to aid robust interpretations.

130 The SISALv3 database will allow the systematic and global analysis of stable isotope and trace element variability, and elucidate how trace element data can be used to strengthen climatic interpretations from speleothem oxygen ($\delta^{18}\text{O}$) and carbon ($\delta^{13}\text{C}$) records. The database can be accessed at <http://dx.doi.org/10.5287/ora-2nanwp4rk>.

Proxy	Potential drivers	Selected relevant references
$\delta^{18}\text{O}$	Semi-quantitative temperature reconstruction dependent on the combined effect of temperature dependency of meteoric precipitation $\delta^{18}\text{O}$ and in-cave temperature on carbonate $\delta^{18}\text{O}$	(Dorale et al., 1998; Mangini et al., 2005; Moseley et al., 2015; Koltai et al., 2017; Wendt et al., 2021; Luetscher et al., 2021; Wolf et al., 2024; Wainer et al., 2011)
	Change in source water composition e.g. as tracers of ice sheet meltwaters during deglaciations	(Stoll et al., 2022; Badertscher et al., 2011; Frumkin et al., 1999; Meckler et al., 2012)
	Change in moisture transport trajectory or change in moisture source (sometimes linked to seasonality)	(Lachniet et al., 2014; Cheng et al., 2016; Luetscher et al., 2021; Frumkin et al., 1999)
	Change in seasonality of precipitation e.g. increase winter rain versus summer rain in different climate states	(Cheng et al., 2009b; Baldini et al., 2019; Cheng et al., 2019; Wang et al., 2001)
	Precipitation amount at the cave site and upstream rainout	(Bar-Matthews et al., 2003; Hu et al., 2008; Cheng et al., 2016; Columbu et al., 2019; Cheng et al., 2013)
	Large-scale circulation and supra-regional climate e.g. the Indian Summer Monsoon	(Cheng et al., 2016; Kathayat et al., 2016)

	Recharge processes and karst flow paths	(Ayalon et al., 1998; Baker et al., 2019; Treble et al., 2022)
$\delta^{13}\text{C}$	Semi-quantitative temperature reconstruction linked to changes in vegetation and soil respiration (requires additional proxies e.g. Mg/Ca)	(Genty et al., 2003, 2006; Lechleitner et al., 2021; Stoll et al., 2022, 2023)
	Vegetation density variability e.g. low vegetation density zones versus high vegetation density zones	(Fohlmeister et al., 2020)
	Metabolic pathway e.g. C3 versus C4 pathway	(Baker et al., 1997)
	Hydroclimate through the prior calcite precipitation mechanism and/or drip rate changes (requires additional proxies e.g. Mg/Ca)	(Johnson et al., 2006; Owen et al., 2016; Carolin et al., 2019b; Fairchild et al., 2000)
Mg/Ca	Hydroclimate through the prior calcite precipitation mechanism and/or drip rate changes, potential for semi-quantitative precipitation reconstruction (requires additional proxies e.g. $\delta^{13}\text{C}$, Sr/Ca and Ba/Ca, and/or cave monitoring data)	(Johnson et al., 2006; Owen et al., 2016; Carolin et al., 2019b; Fairchild et al., 2000; Warken et al., 2018)
	Hydroclimate through dust activity and marine aerosol input (requires additional proxies e.g. Na/Ca, Sr/Ca and Ba/Ca, and/or cave monitoring data)	(Faraji et al., 2023; Carolin et al., 2019b)
	Hydroclimate through water residence time in soil and karst	(Roberts et al., 1998; Treble et al., 2003; Tremaine and Froelich, 2013)
Sr/Ca	Hydroclimate through the prior calcite precipitation mechanism and/or drip rate changes (requires additional proxies e.g. $\delta^{13}\text{C}$, Mg/Ca and Ba/Ca, and/or cave monitoring data)	(Johnson et al., 2006; Owen et al., 2016; Carolin et al., 2019b; Fairchild et al., 2000)
	Aeolian transport (increased confidence in interpretation with $^{87}\text{Sr}/^{86}\text{Sr}$ data)	(Goede et al., 1998)
Ba/Ca	Hydroclimate through the prior calcite precipitation mechanism and/or drip rate changes (requires additional proxies e.g. $\delta^{13}\text{C}$, Mg/Ca and Sr/Ca, and/or cave monitoring data)	(Johnson et al., 2006)
	Growth rate	(Treble et al., 2003)
	Soil mineral weathering	(Riechelmann et al., 2020; Rutledge et al., 2014)

U/Ca	Hydroclimate through the prior aragonite precipitation mechanism and/or drip rate changes (requires additional proxies e.g. $\delta^{13}\text{C}$, Mg/Ca, Ba/Ca and Sr/Ca, and/or cave monitoring data)	(Jamieson et al., 2016)
	Enhanced infiltration via complexes (e.g., uranyl-phosphate) (requires additional proxies e.g. P/Ca)	(Treble et al., 2003)
P/Ca	Biomass cycling including wildfire; enhanced infiltration via complexes	(Huang et al., 2001; Treble et al., 2003; Borsato et al., 2007; McDonough et al., 2022)
Sr isotopes	Hydroclimate through proportional source changes	(Verheyden et al., 2000; Utida et al., 2020)
	Aeolian activity	(Li et al., 2005)

Table 1: Summary of speleothem geochemical proxies included in SISALv3, examples for their possible interpretations, and

135 relevant references.

2 Data and Methods

2.1 New data formatting and processing

All trace elements are reported normalized as ratios with respect to Ca (X/Ca, where X stands for the individual elements) in
 140 units of mmol/mol. In the following manuscript, "trace element" refers to the normalized ratio to Ca. A standardized conversion sheet is used to facilitate conversions from gram to mol units (available in the repository). Sr-isotope data is reported as $^{87}\text{Sr}/^{86}\text{Sr}$ values. For internal consistency, and to facilitate future intercomparison and synthesis studies, the measurement method and reference materials used, and measurement precision are also reported for both trace elements and Sr-isotopes.

Mechanisms relevant to hydroclimate interpretations from speleothems are based on a multi-proxy approach of stable isotopes
 145 and one or more trace element ratios. Therefore, the SISALv3 database structure allows for trace element measurements to be added at the depths of the stable isotope measurements on a given entity. However, between 35 and 86% of the records (depending on element) were measured using in-situ techniques, such as laser ablation inductively coupled plasma mass spectrometry (LA-ICP-MS), and these datasets are typically generated at a higher resolution (10-100 μm) than the stable isotope records (Jochum et al., 2012). These data have been downsampled to the resolution of the stable isotope data for the same speleothem. Downsampling was performed by computing averages (and standard deviations) of the trace element measurements for corresponding stable isotope sampling depths. This implicitly assumes that the same or a (depth-equivalent) parallel sampling track were used for trace elements and stable isotopes and that the isotope sampling was continuous. Downsampling allows the trace element data to be represented by the same depth-age model as the stable isotope record. For records submitted by the authors where the originally published dataset was at higher resolution than reported in the SISAL

155 database, standardized *.txt datafiles are also available in the repository (see section 5.3 on Code and Data accessibility). No
new chronological information or separate age models are reported for these datasets.

2.2 Additional metadata

New metadata fields are included in the Entity table (see database structure; Figure 1) to allow users to select sites with similar environmental conditions and to take account of factors that might influence the interpretation of individual records. These
160 include information on vegetation, land use, land cover, and host rock type above the cave. This information is often missing from publications and was not available from data contributors, so information from data products has been added as additional fields to the database for completeness. Vegetation type and land use information were provided by the original investigators. Additionally, information on land use and land cover was taken from the Copernicus Global Land Service Land Cover database (LCC v3.0.1 Epoch 2019; (Buchhorn et al., 2021, 2020), extracted with a radius of 250 m around the cave site. Information on
165 the carbonate/evaporite host rock at the cave sites was taken from the WOKAM database (Goldscheider et al., 2020) extracted with a radius of 1000 m.

The database also indicates if the trace element content of the host rock and drip water feeding the speleothem is available (but does not include the actual values). Drip height (i.e., the distance the drip falls from the ceiling of the cave to the speleothem), and the difference between dripwater and carbonate $\delta^{18}\text{O}$ values are given, based on information provided by the original
170 investigators.

The SISAL WG repository now hosts images of the entities (speleothem sections) and maps of cave sites. These allow users to evaluate petrographic features that may influence the trace element and stable isotopic records and to check whether cave morphology could potentially influence the climate in the cave (Covington and Perne, 2015). The entity table in the database contains fields indicating whether maps and images are available.

175 2.3 Changes to database structure

The structure of the SISALv3 database (Figure 1) has been changed to accommodate additional data and metadata, and to optimize the organization of information, as described below.

2.3.1 New geochemical data and metadata fields

The elemental ratio for each trace element and the Sr-isotope data are given in individual tables that contain sample identifiers
180 (*sample_id*), the measurement value and the measurement precision. The *sample_id* provides the link to the Sample table and thus links these data to the stable isotope data (Figure 1, Table 2).

Metadata for the measurements are stored in the Entity table. For each elemental ratio (Sr/Ca, Mg/Ca, U/Ca, Ba/Ca and P/Ca), the Entity table indicates whether the data are available (“yes/no/other/unknown”), the measurement method, the laboratory reference materials used and, where applicable, the downsampling methods used. The table also indicates if high-resolution

185 trace element data is available. For Sr-isotopes, the Entity table specifies whether this dataset is available, what measurement method was employed and how the measurement was standardized (Figure 1, Table 2).

SISALv3 now provides a unique, persistent identifier for each speleothem (*persist_id*) in the Entity table (Figure 1, Table 2). This was needed because there was an increasing issue with non-unique entity names, and to deal with the fact that different datasets from the same stalagmite had different *entity_ids* (e.g., for datasets covering different time periods in the same
190 stalagmite). Thus, the field *entity_id* provides a unique identifier for a specific dataset, but not necessarily for a specific speleothem, while the *persist_id* uniquely identifies the speleothem. The *persist_id* were created by combining the *site_id* and *entity_name* (without special characters). There are 838 unique *persist_ids* and 902 unique *entity_ids* in the database.

2.3.2 Changes in existing database fields and options

The fields “geology” and “rock age” were moved from the Site table to the Entity table (Figure 1, Table 2). This was done to
195 allow for variability in these parameters within the same cave system, particularly relevant for the interpretation of $\delta^{13}\text{C}$ and trace element data. The field “trace elements” (yes/no) in the Entity table was removed as it is now redundant. The field “iso_std” describing the reference material used for measurement of $\delta^{18}\text{O}$ and $\delta^{13}\text{C}$ values was moved from the stable isotope tables to the Entity metadata table. A number of options for entries in the metadata fields were changed (Table 3). The majority of these changes were additions to the previously available options in light of the entries made in the ‘Notes’ section to allow
200 for more “metadata-filterable” database mining. A few options were removed from the metadata fields since they have never been used in previous database versions.

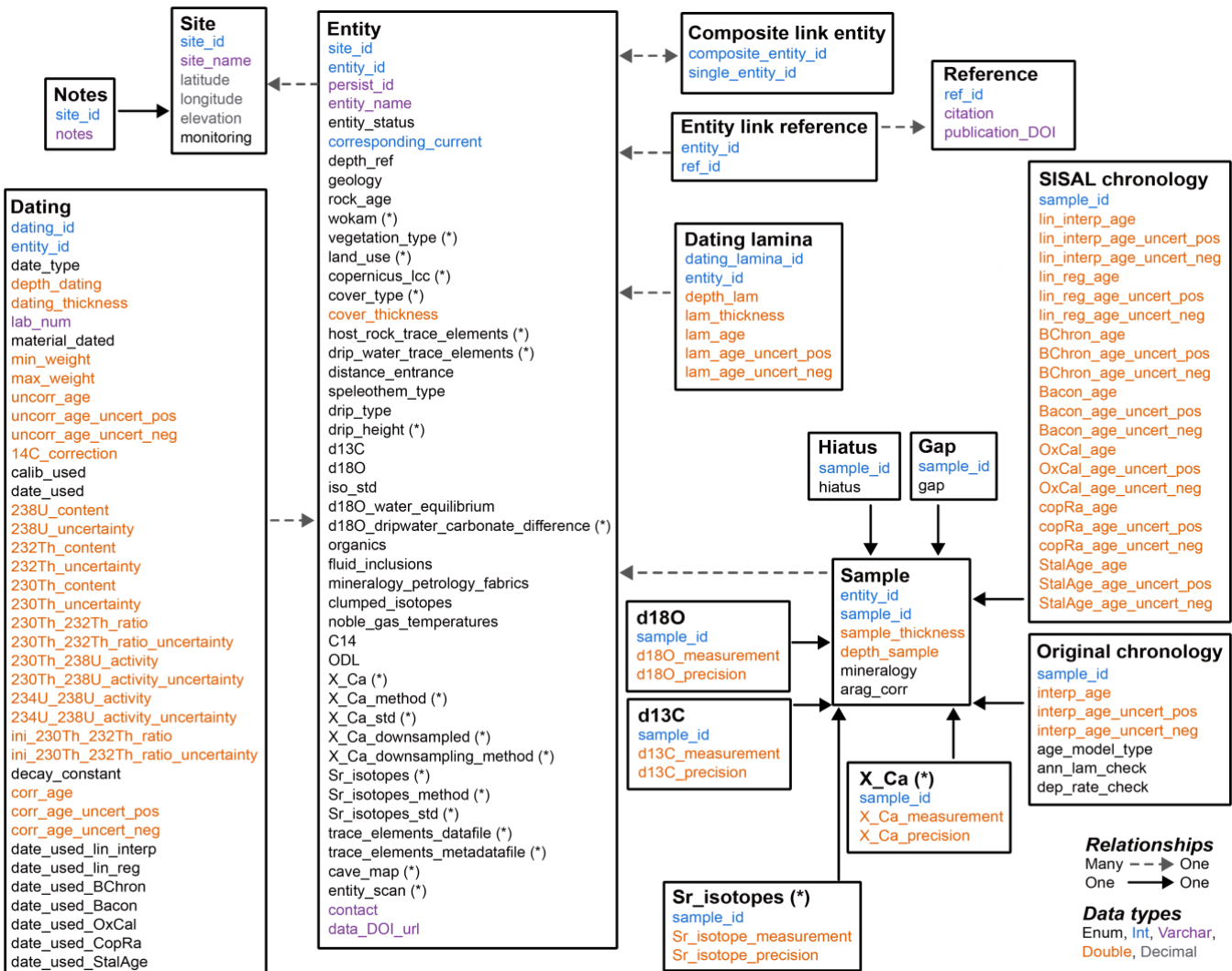


Figure 1: Structure of the SISALv3 database. Fields and tables marked with (*) refer to new information added in SISALv3;

205

see table 2 for details. The colors refer to the format of that field: Enum, Int, Varchar, Double or Decimal. More information on the list of pre-defined menus can be found in the Supplementary information (Table S1). For trace element records, a series of identical tables was generated (labelled X_Ca where X stands for the specific element: Mg, Sr, Ba, U, P).

Action	Field label	Description	Format	Constraints
Changes made to the SITE table				
Field removed	geology			
Field removed	rock_age			

<u>Changes made to the ENTITY table</u>				
Field added	<i>persist_id</i>	persistent, unique identifier for each speleothem	Text	
Field added	<i>geology</i>	Information on geology	Text	Selection from predefined list
Field added	<i>rock_age</i>	Information on bedrock age	Text	Selection from predefined list
Field added	<i>wokam</i>	Information on type of carbonate/evaporite rock from WOKAM database	Text	Added by SISAL SC at database level
Field added	<i>vegetation_type</i>	Information on vegetation cover	Text	Selection from predefined list
Field added	<i>land_use</i>	Information on land use (publication/data contributors)	Text	Selection from predefined list
Field added	<i>copernicus_lcc</i>	Information on land cover from Copernicus land cover classification dataset	Text	Added by SISAL SC at database level
Field added	<i>cover_type</i>	Information on land cover (publication/data contributors)	Text	Selection from predefined list
Field added	<i>host_rock_trace_elements</i>	Indication whether trace element data from the host rock has been measured	Text	Selection from predefined list
Field added	<i>drip_water_trace_elements</i>	Indication whether trace element data from the drip water has been measured	Text	Selection from predefined list
Field added	<i>drip_height</i>	Information on drip height (in m)	Numeric	Free to fill
Field added	<i>iso_std</i>	Information on reference material used for oxygen and carbon isotope measurements	Text	Selection from predefined list
Field added	<i>d18O_dripwater_carbonate_difference</i>	Information on difference between dripwater and carbonate oxygen isotope values	Numeric	Free to fill
Field removed	<i>trace_elements</i>			
Field added	<i>Sr_Ca</i>	Indication whether Sr/Ca data has been measured	Text	Selection from predefined list
Field added	<i>Sr_Ca_method</i>	Information on measurement method for Sr/Ca	Text	Selection from predefined list

Field added	<i>Sr_Ca_std</i>	Information on reference material used for Sr/Ca measurements	Text	Selection from predefined list
Field added	<i>Sr_Ca_downsampled</i>	Information on whether Sr/Ca data had to be downsampled	Text	Selection from predefined list
Field added	<i>Sr_Ca_downsampling_method</i>	Information on downsampling method for Sr/Ca, if applicable	Text	Selection from predefined list
Field added	<i>Mg_Ca_method</i>	Information on measurement method for Mg/Ca	Text	Selection from predefined list
Field added	<i>Mg_Ca_std</i>	Information on reference material used for Mg/Ca measurements	Text	Selection from predefined list
Field added	<i>Mg_Ca_downsampled</i>	Information on whether Mg/Ca data had to be downsampled	Text	Selection from predefined list
Field added	<i>Mg_Ca_downsampling_method</i>	Information on downsampling method for Mg/Ca, if applicable	Text	Selection from predefined list
Field added	<i>Ba_Ca</i>	Indication whether Ba/Ca data has been measured	Text	Selection from predefined list
Field added	<i>Ba_Ca_method</i>	Information on measurement method for Ba/Ca	Text	Selection from predefined list
Field added	<i>Ba_Ca_std</i>	Information on reference material used for Ba/Ca measurements	Text	Selection from predefined list
Field added	<i>Ba_Ca_downsampled</i>	Information on whether Ba/Ca data had to be downsampled	Text	Selection from predefined list
Field added	<i>Ba_Ca_downsampling_method</i>	Information on downsampling method for Ba/Ca, if applicable	Text	Selection from predefined list
Field added	<i>U_Ca</i>	Indication whether U/Ca data has been measured	Text	Selection from predefined list
Field added	<i>U_Ca_method</i>	Information on measurement method for U/Ca	Text	Selection from predefined list
Field added	<i>U_Ca_std</i>	Information on reference used for U/Ca measurements	Text	Selection from predefined list
Field added	<i>U_Ca_downsampled</i>	Information on whether U/Ca data had to be downsampled	Text	Selection from predefined list

Field added	<i>U_Ca_downsampling_method</i>	Information on downsampling method for U/Ca, if applicable	Text	Selection from predefined list
Field added	<i>P_Ca</i>	Indication whether P/Ca data has been measured	Text	Selection from predefined list
Field added	<i>P_Ca_method</i>	Information on measurement method for P/Ca	Text	Selection from predefined list
Field added	<i>P_Ca_std</i>	Information on reference material used for P/Ca measurements	Text	Selection from predefined list
Field added	<i>P_Ca_downsampled</i>	Information on whether P/Ca data had to be downsampled	Text	Selection from predefined list
Field added	<i>P_Ca_downsampling_method</i>	Information on downsampling method for P/Ca, if applicable	Text	Selection from predefined list
Field added	<i>Sr_isotopes</i>	Indication whether Sr isotope data has been measured	Text	Selection from predefined list
Field added	<i>Sr_isotopes_method</i>	Information on measurement method for Sr isotopes	Text	Selection from predefined list
Field added	<i>Sr_isotopes_std</i>	Information on reference material used for Sr isotope measurements	Text	Selection from predefined list
Field added	<i>trace_elements_datafile</i>	Information on whether the original trace elements data is available in the repository	Text	Selection from predefined list
Field added	<i>trace_elements_metadatafile</i>	Information whether original trace element metadata is available in the repository	Text	Selection from predefined list
Field added	<i>cave_map</i>	Information whether a copy of cave map is available in the repository	Text	Selection from predefined list
Field added	<i>entity_scan</i>	Information whether a scan of the speleothem in the repository	Text	Selection from predefined list
Changes made to the d18O and d13C tables				

Field removed	<i>iso_std</i>	Information on reference material used for $\delta^{18}\text{O}$ and $\delta^{13}\text{C}$ measurements	Text	Selection from predefined list
---------------	----------------	---	------	--------------------------------

Table 2: Changes made to the Site, Entity and stable isotope tables compared to SISALv2.

Table name	Action	Field label	Reason	Format	Constraints
Entity	Added "mixed (see notes)" option	<i>speleothem_type</i>	Standardisation of option across fields	Text	Selected from pre-defined list
Entity	Added "other (see notes)" option	<i>speleothem_type</i>	Standardisation of option across fields	Text	Selected from pre-defined list
Entity	Removed "magmatic" option	<i>geology</i>	Not used	Text	Selected from pre-defined list
Entity	Removed "granite" option	<i>geology</i>	Not used	Text	Selected from pre-defined list
Entity	Added "dolomite limestone" option	<i>geology</i>	Machine-readable format option	Text	Selected from pre-defined list
Entity	Added "marly limestone" option	<i>geology</i>	Machine-readable format option	Text	Selected from pre-defined list
Entity	Added "calcarenite" option	<i>geology</i>	Machine-readable format option	Text	Selected from pre-defined list
Entity	Added "other (see notes)" option	<i>geology</i>	Option to include free text in notes	Text	Selected from pre-defined list
Entity	Added "other (see notes)" option	<i>rock_age</i>	Option to include free text in notes	Text	Selected from pre-defined list
Entity	Added "mixed (see notes)" option	<i>rock_age</i>	Reflect overburden with rocks of different ages	Text	Selected from pre-defined list
Entity	Removed "mixture"	<i>drip_type</i>	Replaced with "mixed (see notes)" option	Text	Selected from pre-defined list
Entity	Removed "not applicable"	<i>drip_type</i>	Not used	Text	Selected from pre-defined list
Entity	Added "mixed (see notes)" option	<i>drip_type</i>	Standardisation of option across fields	Text	Selected from pre-defined list

Entity	Added "other (see notes)" option	<i>drip_type</i>	Option to include free text in notes	Text	Selected from pre-defined list
Entity	Added "other (see notes)" option	<i>d18O_water_equilibrium</i>	Option to include free text in notes	Text	Selected from pre-defined list
Entity	Added "other (see notes)" option	<i>organics</i>	Option to include free text in notes	Text	Selected from pre-defined list
Entity	Added "other (see notes)" option	<i>fluid_inclusions</i>	Option to include free text in notes	Text	Selected from pre-defined list
Entity	Added "other (see notes)" option	<i>mineralogy_petrology_fabric</i>	Option to include free text in notes	Text	Selected from pre-defined list
Entity	Added "other (see notes)" option	<i>clumped_isotopes</i>	Option to include free text in notes	Text	Selected from pre-defined list
Entity	Added "other (see notes)" option	<i>noble_gas_temperatures</i>	Option to include free text in notes	Text	Selected from pre-defined list
Entity	Added "other (see notes)" option	<i>C14</i>	Option to include free text in notes	Text	Selected from pre-defined list
Entity	Added "other (see notes)" option	<i>ODL</i>	Option to include free text in notes	Text	Selected from pre-defined list
Dating	Added "mixed (see notes)" option	<i>material_dated</i>	Align with options in the sample table	Text	Selected from pre-defined list
Dating_lamina	Added "Year of chemistry" option	<i>modern_reference</i>	Align with options in the dating table	Text	Selected from pre-defined list
Sample	Removed "secondary calcite" option	<i>mineralogy</i>	Not used	Text	Selected from pre-defined list
Sample	Removed "vaterite" option	<i>mineralogy</i>	Not used	Text	Selected from pre-defined list
Sample	Added "organic" option	<i>mineralogy</i>	Addition of option	Text	Selected from pre-defined list
Sample	Added "other (see notes)" option	<i>mineralogy</i>	Option to include free text in notes	Text	Selected from pre-defined list
Sample	Removed "combination of methods" option	<i>age_model_type</i>	Standardisation of option across fields	Text	Selected from pre-defined list

Sample	Added "mixed (see notes)" option	<i>age_model_type</i>	Standardisation of option across fields	Text	Selected from pre-defined list
Sample	Added "other (see notes)" option	<i>dep_rate_check</i>	Option to include free text in notes	Text	Selected from pre-defined list

Table 3: Changes made to the predefined options for metadata fields compared to SISALv2.

3 Quality control

The SISAL WG has used several levels of quality control (QC) and this practice was continued for SISALv3 (Figure 2). The initial data compilation is performed by SISAL regional coordinators and/or in liaison with the data contributors into

215 standardized excel workbooks. The first QC level consists in the expert assessment by the SISAL regional coordinators who double-check completeness of entered data and correctness of measurement units where applicable. Standardized unit conversion sheets for common conversions (e.g. degrees-minutes-seconds to decimal degrees for site information; atomic ratios to activity ratios for dating information; mg/g to mmol/mol for trace element-to-Ca ratios for trace element information) have been provided to regional coordinators (see repository). The completed workbook(s) are subjected to a series of automated

220 QC (e.g., age model matches discreet dating information, hiatuses are placed at the correct depth) by the database managers. When the datasets pass automated QC, and no further corrections are necessary, the dataset workbook and auto generated QC figures are sent to the data contributors for final evaluation and approval. The same workflow has been followed for the *.txt trace element datafiles. The new metadata fields of vegetation_type and land_use that have been added to SISALv3 for entities that were included in SISALv2 from publications. Data already included in SISALv2 has been checked, and mistakes /

225 unknowns identified during previous data analysis or during the process of trace element data addition were corrected. A comprehensive summary of the changes made to existing entities between SISALv2 and SISALv3 is shown in Table 4.

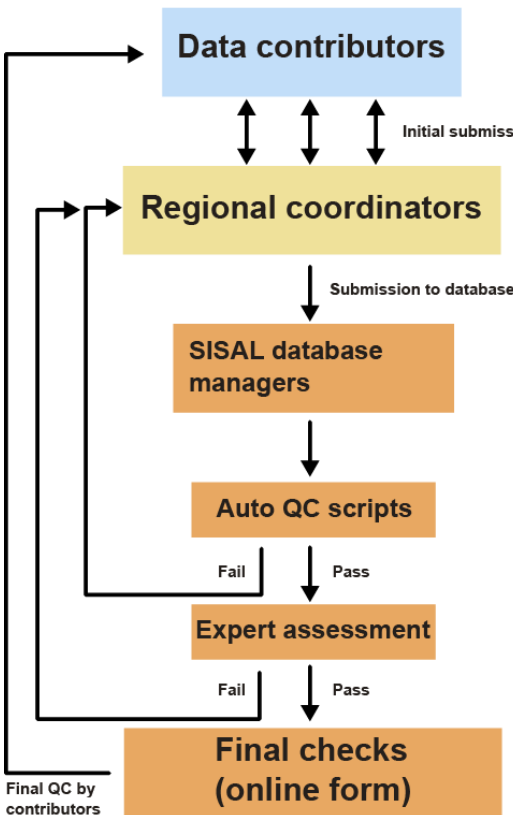


Figure 2: Quality checking workflow adopted for inclusion of datasets in SISAL. The colors indicate different quality check levels: blue - data contributing sources (original authors or datasets deposited in repositories and publication supplementary information); yellow - SISAL regional coordinator group with regional expertise; orange - SISAL database managers.

Modification	v2 to v3
Site table	
Number of new sites	72
Pre-existing sites with new entities	37
Entity table	
Number of new entities	211
Entities added to pre-existing sites	71
Entities with updated entity.entity_status	33
Entities with altered entity.corresponding_current	1
Entities with altered geology	106

Entities with altered rock_age	58
Entities with altered entity.cover_thickness	6
Entities with altered distance_entrance	1
Entities with altered d13C	109
Entities with altered d18O	15
Entities with altered organics	9
Entities with altered fluid_inclusions	9
Entities with altered mineralogy_petrology_fabric	14
Entities with altered clumped_isotopes	9
Entities with altered noble_gas_temperatures	12
Entities with altered C14	3
Entities with altered ODL	7
Entities with altered contact	62
Entities with altered data_DOI_url	20
Dating table	
Addition of "event: hiatus" to an entity	1
Changes in hiatus depths	1
Changes in depths of "Event: start/end of laminations"	1
Alterations in dating.date_type	2
Alterations in dating.depth_dating	5
Alterations in dating.material_dated	2
Alterations in dating.min_weight	6
Alterations in dating.max_weight	6
Alterations in dating.uncorr_age	15
Alterations in dating.uncorr_age_uncert_pos	13
Alterations in dating.uncorr_age_uncert_neg	13
Alterations in dating.date_used	27
Alterations in dating.238U_content	89
Alterations in dating.238U_uncertainty	34
Alterations in dating.232Th_content	96
Alterations in dating.232Th_uncertainty	85
Alterations in dating.230Th_232Th_ratio	206
Alterations in dating.230Th_232Th_ratio_uncertainty	200
Alterations in dating.230Th_238U_activity	24

Alterations in dating.230Th_238U_activity_uncertainty	21
Alterations in dating.234U_238U_activity	381
Alterations in dating.234U_238U_activity_uncertainty	433
Alterations in dating.ini_230Th_232Th_ratio	519
Alterations in dating.ini_230Th_232Th_ratio_uncertainty	485
Alterations in dating.decay_constant	77
Alterations in dating.corr_age	71
Alterations in dating.corr_age_uncert_pos	26
Alterations in dating.corr_age_uncert_neg	28
Sample table	
Altered sample.depth_sample	1084
Altered sample.mineralogy	294
Altered sample.arag_corr	294
Entities that had d18O time series altered (changes in depth/ duplicate isotope values)	4
Entities that had d13C time series altered (changes in depth/ duplicate isotope values)	2
Original chronology	
Altered original_chronology.interp_age	7440
References	
How many entities had changes in references?	100
How many citations have a different pub_DOI?	100
Notes	
Sites with notes modified	121

Table 4: Summary of the modifications applied to records in version 2 (Comas-Bru et al., 2020) of the SISAL database. Note that the changes in the dating and sample table were counted by dating_id and sample_id, respectively, which leads to a large number of changes.

4 Overview of database contents

4.1 Trace element and Sr-isotope records

SISALv3 contains 95 Mg/Ca, 85 Sr/Ca, 52 Ba/Ca, 25 U/Ca, 29 P/Ca and 14 Sr-isotope records (Table 5). This corresponds to

240 ~60% of the known published data, based on an assessment by the SISAL WG. There is a clear regional bias in the database with European entities dominating every elemental ratio (Figure 3). The Sr-isotope records are more evenly distributed, with records from every region except Asia and Oceania. Temporal coverage for the combined trace element and Sr-isotope dataset is high during the last 2000 years (~60 entities per 20 year interval) and the Holocene (~60 entities per 250 year interval), and then drops to 20-40 entities per 10,000 year interval for the last glacial cycle (12-120 ka BP, where ka stands for 1000 years
245 and BP for "before present", defined as 1950, Figure 4). Beyond ~120 ka BP, the number of entities gradually decreases until the U-Th dating limit is reached (~640 ka).

Where the original measured laser ablation data have been provided by data contributors, these have been made available as *.txt datafiles in the repository (Table 5). Forty-six trace element records (Mg/Ca: 15, Sr/Ca: 17, Ba/Ca: 4, U/Ca: 5, P/Ca: 5, Sr-isotopes: 2) are only provided in the original format (*.txt files), either because they could not be converted to mmol/mol
250 or because the trace element data were not measured at stable isotope equivalent depths and were at an insufficiently high resolution for accurate resampling. Additional elements that are not included in the database, but have been submitted by data contributors, are also provided as *.txt files (e.g., Mn, Fe, Zn, Th, Pb, K, Na).

Geochemical data	Total number in SISAL	Downsampled by original authors	Downsampled by SISAL	Only in repository
Mg/Ca	95	12	15	15
Sr/Ca	85	11	11	17
Ba/Ca	52	11	9	4
U/Ca	25	2	6	5
P/Ca	29	4	12	5

Table 5: Summary of number of trace element records in SISAL and downsampling methods applied.

255

4.2 New stable isotope records

SISALv3 provides a significantly expanded oxygen isotope dataset compared to SISALv2 (Table 6, Table 7, Figure 5), with 892 $\delta^{18}\text{O}$ records from 365 sites, compared to 673 records in SISALv2. The most significant increases in $\delta^{18}\text{O}$ records are in Africa (+28 records), Europe (+73), and the Middle-East (+17; Table 6). SISALv3 contains 334 entities covering the last 2000

260 years, of which 78 are new (Figure 6). As record density begins to decrease with age (Figure 6), the spatial distribution is reduced as well. For the Last Glacial Maximum (20 – 22 ka BP), SISALv3 contains 92 entities (11 new), while for the Last Interglacial (124 – 126 ka BP), 66 entities are available (15 new). Four $\delta^{18}\text{O}$ records previously included in SISALv2 have been modified to correct previous mistakes (Table 4), these are *entity_ids* 110 (CUR4; Novello et al., 2016), 169 (Dim-E3; Ünal-İmer et al., 2015), 447 (JAR4; Novello et al., 2017), and 573 (Gej-1; Flohr et al., 2017).

265 There has also been a significant increase in the number of $\delta^{13}\text{C}$ records added, with 620 records in SISALv3 compared to 430 in SISALv2 (Table 6, Figure 7). At the regional scale, the most significant increases in $\delta^{13}\text{C}$ records is for Africa (+23 records), Asia (+33), and Europe (+66, Table 6). The $\delta^{13}\text{C}$ record coverage decreases following the same patterns as the trace elements and $\delta^{18}\text{O}$ records (Figure 8). Two $\delta^{13}\text{C}$ records previously included in SISALv2 have been modified to correct previous mistakes (Table 4), these are *entity_ids* 169 (Dim-E3; Ünal-İmer et al., 2015), and 573 (Gej-1; Flohr et al., 2017).

270

Region	$\delta^{18}\text{O}$ records in v3	Increase compared to v2 (counts)	$\delta^{13}\text{C}$ records in v3	Increase compared to v2 (counts)
Africa	73	28	63	23
Asia	237	50	105	33
Europe	243	73	213	66
Middle East	60	17	43	14
Oceania	100	11	66	11
North and Central America	88	9	72	9
South America	97	21	54	13

Table 6: Summary of the new $\delta^{18}\text{O}$ and $\delta^{13}\text{C}$ records added to SISALv3 compared to SISALv2.

site_id	site_name	region	latitude	longitude	persist_id	entity_id	entity_name	citation
70	Abaco Island cave	Bahamas	26.23	-77.16	70-ABDC12	692	AB-DC-12_2023	(Arienzo et al., 2017)
79	Dim cave	Turkey	36.53 4	32.105 6	79-DIME4	693	Dim-E4_2023	(Ünal-İmer et al., 2016, 2015)

					79-DIM1	754	Dim1	(Rowe et al., 2020)
144	Botuverá cave	Brazil	- 27.22 47	- 49.156 9	144-BT2	694	BT-2_2007	(Cruz et al., 2007)
145	Antro del Corchia	Italy	43.98 33	10.216 7	145-CD31	695	CD3-1_HR	(Drysdale et al., 2020)
						696	CD3-1_LR	(Drysdale et al., 2020)
266	Cueva Victoria	Spain	37.63 22	- 0.8215	266-VICIII1	697	Vic-III-1	(Budsky et al., 2019; Ros and Llamusí, 2012)
					266-VICIII3	698	Vic-III-3	(Budsky et al., 2019; Ros and Llamusí, 2012)
					266-SR01T	699	SR01t	(Budsky et al., 2019; Ros and Llamusí, 2012)
39	Dongge cave	China	25.28 33	108.08 33	39-D3	700	D3_2005	(Kelly et al., 2006)
					39-D4	701	D4_2005_Kelly	(Kelly et al., 2006)
120	Ejulve cave	Spain	40.76	-0.59	120- ANDROMEDA	702	Andromeda	(Pérez-Mejías et al., 2019)
192	El Condor cave	Peru	-5.93	-77.3	192-ELCB	703	ELC-B_2021	(Cheng et al., 2021)
115	Hölloch im Mahdtal	Austria	47.37 81	10.150 6	115-HOL1	704	HOL1	(Li et al., 2021a)
					115-HOL22	705	HOL22	(Li et al., 2021a)
6	Hulu cave	China	32.5	119.17	6-MSL	706	MSL_2021	(Cheng et al., 2021)
10	Jaraguá cave	Brazil	- 21.08 3	- 56.583	10-JAR2	707	JAR2	(Novello et al., 2019)
24	Lapa sem fim cave	Brazil	- 16.15 03	- 44.628 1	24-LSF13	708	LSF13_2018	(Stríkis et al., 2018)

					24-LSF19	709	LSF19	(Azevedo et al., 2021)
					24-LSF17	710	LSF17	(Azevedo et al., 2021)
					24-LSF13	711	LSF13_2021	(Cheng et al., 2021)
3	Paraiso cave	Brazil	-4.0667	-55.45	3-PAR27	712	PAR27	(Cheng et al., 2021)
					3-PAR15	713	PAR15	(Cheng et al., 2021)
268	Pere Noel cave	Belgium	50	5.2	268-PN955	714	PN-95-5_2018	(Allan et al., 2018)
								Allan et al. (2018)
87	Pindal cave	Spain	43.4	-4.53	87-CANDELA	715	Candela_2023	(Moreno et al., 2010)
						716	Candela_Base	(Stoll et al., 2022)
						717	Candela_Main	(Stoll et al., 2022)
						718	Candela_L	(Stoll et al., 2022)
					87-LAURA	719	Laura	(Stoll et al., 2022)
295	Qadisha cave	Lebanon	34.2439	30.0364	295-QAD1	720	Qad_1	(Nehme et al., 2023)
					295-QAD2	721	Qad_2	(Nehme et al., 2023)
232	Rio Secreto cave system	Mexico	20.59	-87.13	232-RS1	722	RS1	(Serrato Marks et al., 2021)
219	Shennong cave	China	28.71	117.26	219-SN35	723	SN35	(Zhang et al., 2021a)
					219-SN31	724	SN31	(Zhang et al., 2021a)
					219-SN29	725	SN29	(Zhang et al., 2021a)
					219-SN-COMP	726	SN_composite	(Zhang et al., 2021a)

					219-SN17	727	SN17_2021	(Zhang et al., 2021a)
55	Sieben Hengste cave	Austria	46.75	7.81	55-7H12	728	7H-12	(Luetscher et al., 2021)
58	Spannagel cave	Austria	47.08	11.67	58-SPA121	729	SPA121_2021	(Wendt et al., 2021)
					58-SPA146	730	SPA146	(Wendt et al., 2021)
					58-SPA183	731	SPA183	(Wendt et al., 2021)
					58-SPA127	732	SPA127_2023	(Fohlmeister et al., 2013; Welte et al., 2021)
279	Staircase cave	South Africa	- 34.20 71	22.089 9	279-STAIRCASE-COMP	733	Staircase_composite	(Braun et al., 2019b)
236	Toca da Boa Vista	Brazil	- 10.16 02	- 40.860 5	236-TBV5	734	TBV5	(Cheng et al., 2021)
					236-TBV13	735	TBV13	(Zhang et al., 2021c)
69	Xinglong cave	China	40.5	117.5	69-XL4	736	XL-4	(Duan et al., 2019, 2022)
296	Amir Timur cave	Uzbekistan	39.42 27	66.763 2	296-S124	737	S-12-4	(Finestone et al., 2022)
94	Anjohibe	Madagascar	- 15.53	46.88	94-ABC1	738	ABC-1	(Li et al., 2020)
297	Bàsura cave	Italy	44.13	8.2	297-BA184	739	BA18-4	(Hu et al., 2022)
298	Belum cave	India	15.1	78.1	298-BLM1	740	BLM-1	(Band et al., 2022)
299	Calabrez	Spain	43.45	-5.13	299-ALICIA	741	Alicia	(Stoll et al., 2022)
300	Careys cave	Australia	- 35.07	148.66	300-CC146	742	CC14-6	(Scroxton et al., 2021)
301	Cathedral cave	Australia	- 32.61 7	148.94	301-WB	743	WB	(Markowska et al., 2020)
					301-WC	744	WC	(Markowska et al., 2020)

302	Crevice cave	South Africa	-34.21	22.09	302-CREVICE-COMP	745	Crevice_composite	(Bar-Matthews et al., 2010)
303	Crystal cave, Australia	Australia	-34.1	115	303-CRYS1	746	CRY-S1	(Priestley et al., 2023; Treble et al., 2003)
304	Cueva Bonita	Mexico	23	-99	304-CB4	747	CB4	(Wright et al., 2022)
305	Cueva Rosa	Spain	43.44 36	-5.1403	305-NEITH	748	Neith_2022	(Stoll et al., 2022)
						749	Neith_2015	(Stoll et al., 2015)
					305-ARTEMISAR	750	Artemisa_R	(Stoll et al., 2015)
					305-ANGELINES	751	Angelines	(Stoll et al., 2015)
306	Cuica cave	Brazil	-11.68 22	-60.643 1	306-PIM4	752	PIM4	(Della Libera et al., 2022)
					306-PIM5	753	PIM5	(Della Libera et al., 2022)
307	Efflux cave	South Africa	-33.41	22.34	307-EFFLUX-COMP	755	Efflux_composite	(Braun et al., 2020)
					307-142843	756	142843	(Braun et al., 2020)
					307-142846	757	142846	(Braun et al., 2020)
					307-142847	758	142847	(Braun et al., 2020)
					307-142848	759	142848	(Braun et al., 2020)
					307-142849	760	142849	(Braun et al., 2020)
308	GD8	Greenland	80.37 77	-21.746 8	308-GD81SLAB1	761	GD8-1 Slab 1	(Moseley et al., 2021)
					308-GD81SLAB1ORB	762	GD8-1 Slab 1 orb	(Moseley et al., 2021)
					308-GD81SLAB2	763	GD8-1 Slab 2	(Moseley et al., 2021)
309	Goda Mea cave	Ethiopia	9.49	37.66	309-GM1	764	GM1	(Asrat et al., 2018)

310	Golgotha cave	Australia	-34.083	115.05	310-GLS1	765	GL-S1	(Treble et al., 2022)
					310-GLS2	766	GL-S2	(Treble et al., 2022)
					310-GLS3	767	GL-S3	(Treble et al., 2022)
					310-GLS4	768	GL-S4	(Treble et al., 2022)
311	Harrie Wood cave	Australia	-35.7	148.5	311-HWS1	769	HW-S1	(Tadros et al., 2022, 2016)
					311-HWS2	770	HW-S2	(Tadros et al., 2022, 2016)
					311-HW38B	771	HW_38b	(Tadros et al., 2022, 2016)
312	Heifeng cave	China	29.0167	107.1833	312-HF01	772	HF01	(Yang et al., 2019)
313	Herbstlabyrinth cave	Germany	50.6875	8.2058	313-HLK2	773	HLK2	(Waltgenbach et al., 2020)
					313-NG01	774	NG01	(Waltgenbach et al., 2021)
					313-TV1	775	TV1_2021	(Waltgenbach et al., 2021)
						776	TV1_2020	(Waltgenbach et al., 2020)
314	Herolds Bay cave	South Africa	-34.05	22.39	314-HEROLDSBAY-COMP	777	Herolds_bay_composite	(Braun et al., 2020)
					314-162520	778	162520	(Braun et al., 2020)
					314-1625271	779	162527-1	(Braun et al., 2020)
					314-162528	780	162528	(Braun et al., 2020)
					314-1625272	781	162527-2	(Braun et al., 2020)
315	Huangchao cave	China	36.6167	118.3333	315-HC2	782	HC2	(Tan et al., 2020a)
316	Hüttenbläaserschachhöhle	Germany	51.3689	7.6547	316-HBSH1	783	HBSH-1	(Weber et al., 2021)

					316-HBSH3	784	HBSH-3	(Weber et al., 2021)
					316-HBSH4	785	HBSH-4	(Weber et al., 2021)
					316-HBSH5	786	HBSH-5	(Weber et al., 2021)
42	Ifoulki cave	Morocco	30.70 8	- 9.3275	42-IFK2	787	IFK2	(Sha et al., 2021)
317	Jiangjun cave	China	22.95	104.81 67	317-JJ0406	788	JJ0406	(Wassenburg et al., 2021; Liu et al., 2020)
					317-JJ0403	789	JJ0403	(Wassenburg et al., 2021; Liu et al., 2020)
318	Jinfo cave	China	29.01 67	107.17 92	318-J12	790	J12	(Yang et al., 2019)
					318-J13	791	J13	(Yang et al., 2019)
319	Jiulong cave	China	27.8	113.9	319-JL1	792	JL1	(Zhang et al., 2021b)
320	Katalekhор	Iran	35.85	48.16	320-KT3	793	KT-3	(Andrews et al., 2020)
100	Katerloch cave	Austria	47.08 33	15.55	100-K2	794	K2	(Honiat et al., 2022)
					100-K4	795	K4	(Honiat et al., 2022)
321	Klang	Thailand	8.33	98.73	321-TK7	796	TK7	(Chawchari et al., 2021)
					321-TK20	797	TK20	(Chawchari et al., 2021)
					321-TK40	798	TK40	(Chawchari et al., 2021)
322	Kuna Ba	Iraq	35.09	45.38	322-NIR1	799	NIR-1	(Sinha et al., 2019)
					322-NIR2	800	NIR-2	(Sinha et al., 2019)
					322-NIR-COMP	801	NIR_composite	(Sinha et al., 2019)
323	Kyok-Tash cave	Russia	51.72 9	85.656	323-K4KYOK	802	K4_kyok	(Li et al., 2021b)

324	La Vallina	Spain	43.41	- 4.8067	324-GAEL	803	Gael_2022	(Stoll et al., 2022)
						804	Gael_2015	(Stoll et al., 2015)
					324-GLORIA	805	Gloria	(Stoll et al., 2015)
					324-GARTH	806	Garth	(Stoll et al., 2022)
					324-GULDA	807	Gulda	(Stoll et al., 2022)
					324-LUNA	808	Luna	(Stoll et al., 2022)
					324-GALIA	809	Galia	(Stoll et al., 2022)
221	La Vierge cave	Mauritius	- 19.75 72	63.370 3	221-LAVI157	810	LAVI-15-7	(Li et al., 2020)
					221-LAVI4	811	LAVI-4_2020	(Li et al., 2020)
325	Larga cave	Puerto Rico	18.32	-66.8	325-PRLA1	812	PR-LA-1	(Warken et al., 2020)
326	Linzhu cave	China	31.51 67	110.31 67	326-LZ15	813	LZ15	(Cheng et al., 2009a)
					326-LZ36	814	LZ36	(Cheng et al., 2009a)
327	Manita peć cave	Croatia	45.31 42	15.475 4	327-MP2	815	MP-2	(Surić et al., 2021b)
					327-MP3	816	MP-3	(Surić et al., 2021b)
328	Mata Virgem cave	Brazil	- 11.62	-47.49	328-MV3	817	MV3	(Azevedo et al., 2019)
329	Matupi cave	Democratic Republic of Congo	1.25	29.82	329-MAT1	818	MAT1	(Dupont et al., 2022)
					329-MAT12	819	MAT12	(Dupont et al., 2022)
					329-MAT23	820	MAT23	(Dupont et al., 2022)
330	Meravelles cave	Spain	40.94 88	0.5127	330-MAAT	821	Maat	(Pérez-Mejías et al., 2021)

331	Mizpe Shelagim	Mount Hermon (Levant)	33.32	35.81	331-MS-COMP	822	MS-composite	(Ayalon et al., 2013)
					331-MS1	823	MS-1	(Ayalon et al., 2013)
					331-MS2	824	MS-2	(Ayalon et al., 2013)
					331-MS3	825	MS-3	(Ayalon et al., 2013)
332	Murada	Spain	39.95 6	3.965	332-INDIANA	826	Indiana	(Torner et al., 2019)
333	Neotektonik cave	Switzerland	46.78 33	8.2667	333-M37116A	827	M37-1-16A	(Wilcox et al., 2020)
					333-M37116C	828	M37-1-16C	(Wilcox et al., 2020)
					333-M37123A	829	M37-1-23A	(Wilcox et al., 2020)
334	Nova Grgosova cave	Croatia	45.81 88	15.678 3	334-NG7	830	NG-7	(Surić et al., 2021a)
					334-NG3	831	NG-3	(Surić et al., 2021a)
335	Ostolo cave	Spain	43.18 78	- 0.2678	335-OST2	832	OST2	(Bernal-Wormull et al., 2021)
					335-OST1	833	OST1	(Bernal-Wormull et al., 2021)
					335-OST3	834	OST3	(Bernal-Wormull et al., 2021)
336	Pentadactylos	Cyprus	35.27	33.47	336-PENTADACTYLOS1	835	Pentadactylos-1	(Nehme et al., 2020)
337	Pir Ghar cave	Iran	35.23	57.42	337-PG113	836	PG11-3	(Carolin et al., 2019a)
338	Coves del pirata	Spain	39.50 46	3.3009	338-CONSTANTINE	837	Constantine	(Cisneros et al., 2021)

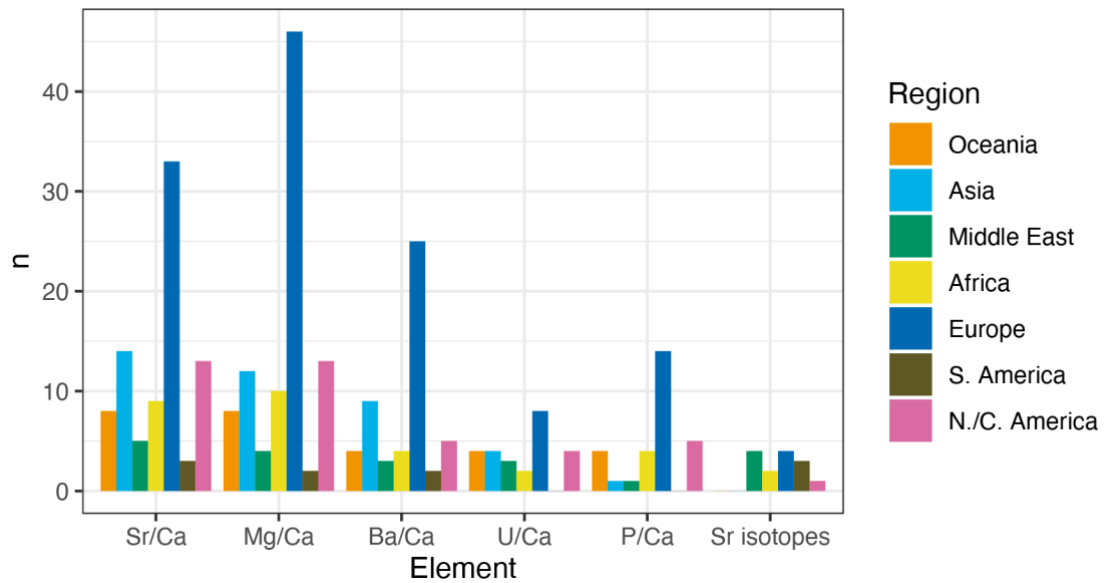
339	Pozzo Cucù cave	Italy	40.9	17.16	339-PC	838	PC	(Columbu et al., 2020)
254	PP29	South Africa	- 34.20 78	22.087 6	254-PP29-COMP	839	PP29_composite	(Braun et al., 2019b)
340	Qujia cave	China	35.7	118.4	340-QJ1	840	QJ1	(Zhao et al., 2021)
341	Rey Marcos	Guatema la	15.42 77	- 90.280 7	341-GURM1	841	GU-RM-1	(Winter et al., 2020)
342	Sa balma des Quartó cave	Spain	39.51 45	3.3059	342-SEAN	842	Seán	(Cisneros et al., 2021)
					342-MULTIEIX	843	Multieix	(Cisneros et al., 2021)
					342-CIARA	844	Ciara	(Cisneros et al., 2021)
					342-FENI	845	Feni	(Cisneros et al., 2021)
140	Sanbao cave	China	31.66 7	110.43 33	140-SB61	846	SB61	(Cheng et al., 2009a)
343	Sant'Angelo cave	Italy	40.7	17.5	343-SA1	847	SA1	(Columbu et al., 2022)
345	Schratten cave	Switzerla nd	46.78 33	8.2667	345-M6733	849	M6-73-3	(Wilcox et al., 2020)
20	Secret cave	Borneo	4.084 8	114.85 03	20-SC02	850	SC02_2022	(Buckingham et al., 2022)
346	Shijiangjun cave	China	26.2	105.5	346-SJJ7	851	SJJ7	(Chen et al., 2021)
347	Shizi cave	China	29.68 22	106.28 81	347-QM09	852	QM09	(Yang et al., 2019)
348	Sudwala cave	South Africa	- 25.37	20.7	348-SC1	853	SC1	(Green et al., 2015)
349	Talisman cave	Kyrgyzstan	40.39	72.35	349-F11	854	F11	(Tan et al., 2021)
					349-F2TALISMAN	855	F2_Talisman	(Tan et al., 2021)
293	Tham Doun Mai	Laos	20.75	102.65	293-TM5	856	TM5	(Griffiths et al., 2020)

				102.65	293-TM4	857	TM4	(Griffiths et al., 2020)
				102.65	293-TM11	858	TM11	(Griffiths et al., 2020)
350	Toca da Barriguda	Brazil	- 10.16	-40.86	350-TBR14	859	TBR14	(Wendt et al., 2019)
					350-TBR1013	860	TBR10-13	(Cheng et al., 2021)
351	Trapiá cave	Brazil	-5.6	-37.7	351-TRA7	861	TRA7	(Utida et al., 2020)
352	War Eagle	United States of America	34.67	-86.05	352-PPNDA	862	PPnda	(Medina-Elizalde et al., 2022)
250	Wuya cave	China	33.82	105.43	250-WY12	863	WY12	(Tan et al., 2020b)
					250-WY13	864	WY13	(Tan et al., 2020b)
					250-WY14	865	WY14	(Tan et al., 2020b)
					250-WY56	866	WY56	(Tan et al., 2020b)
353	Wintimdouine	Morocco	30.77	-9.49	353-WIN1	867	WIN1	(Sha et al., 2019)
					353-WIN2	868	WIN2	(Sha et al., 2021, 2019)
					353-WIN3	869	WIN3	(Sha et al., 2021, 2019)
					353-WIN-COMP	870	WIN_composite	(Sha et al., 2019)
354	Wulu cave	China	26.05	105.08 33	354-WULU30	871	Wulu-30	(Cheng et al., 2021; Liu et al., 2018)
					354-WU88	872	Wu88	(Liu et al., 2023, p.202)
					354-WU37	873	Wu37	(Zhao et al., 2020)
355	Xiniu cave	China	31.51 67	110.57	355-XN2	874	XN2	(Zhao et al., 2021)

				110.57	355-XN15	875	XN15	(Zhao et al., 2021)
				110.57	355-XN-COMP	876	XN_composite	(Zhao et al., 2021)
5	Yangkou cave	China	29.03 33	107.18 33	5-JFYK2	877	JFYK2	(Zhang et al., 2021b)
356	Yangzi cave	China	29.78 3	107.78 3	356-YZ1	878	YZ1	(Wu et al., 2020)
357	Yonderup cave	Australia	- 31.54 7	115.69	357-YDS2	879	YD-S2	(McDonough et al., 2022; Nagra et al., 2017, 2016)
358	Zhangjia cave	China	32.58 33	105.08 33	358-ZJD171	880	ZJD171	(Cheng et al., 2021)
359	Zoolithen cave	Germany	49.77 93	11.282 9	359-ZOOREZ1	881	Zoo-rez-1	(Riechelmann et al., 2019, 2020)
					359-ZOOREZ2	882	Zoo-rez-2	(Riechelmann et al., 2019, 2020)
360	Bigonda cave	Italy	46.01 8	11.581	360-BG2	883	BG2	(Johnston et al., 2021)
					360-BG4	884	BG4	(Johnston et al., 2021)
117	Bunker cave	Germany	51.36 75	7.6647	117-BU1	885	Bu1_2021	(Waltgenbach et al., 2021)
					117-BU4	886	Bu4_2021	(Waltgenbach et al., 2021, 2020)
361	Kocain cave	Turkey	37.23 25	30.711 7	361-KO1	887	Ko-1	(Jacobson et al., 2021)
362	Labyrinth cave	Australia	-34.3	115.1	362-LABS1	888	LAB-S1	(Nagra et al., 2017; Priestley et al., 2023)
363	Lake Shasta cave	United States of America	40.80 4	- 122.30 4	363-LSC2	889	LSC2	(Oster et al., 2020)

					363-LSC3	890	LSC3	(Oster et al., 2020)
12	Mawmluh cave	India	25.26 22	91.881 7	12-MAW3	891	MAW-3	(Magiera et al., 2019)
364	Naharon	Mexico	20.18	-87.54	364-NAH14	892	NAH14	(Warken et al., 2021)
365	Pot au Feu	Spain	42.52	0.24	365-JUD	893	JUD	(Torner et al., 2019)
366	Savi cave	Italy	45.61 67	13.883 3	366-SV1	894	SV1	(Belli et al., 2013, 2017)
					366-SV7	895	SV7	(Belli et al., 2013, 2017)
205	São Bernardo cave	Brazil	- 13.81	-46.35	205-SBE3	896	SBE3_2021	(Novello et al., 2018, 2021)
225	Chiflonkhakha cave	Bolivia	- 18.12 22	- 65.773 9	225-BOTO1	897	Boto 1_2021	(Apaéstegui et al., 2018; Novello et al., 2021)
					225-BOTO3	898	Boto 3_2021	(Apaéstegui et al., 2018; Novello et al., 2021)
					225-BOTO7	899	Boto 7_2021	(Apaéstegui et al., 2018; Novello et al., 2021)
54	Sahiya cave	India	30.6	77.866 7	54-SAHA	900	SAH-A_2023	(Sinha et al., 2015)
					54-SAHB	901	SAH-B_2023	(Sinha et al., 2015)
					54-SAHAB-COMP	902	SAH-AB_2023	(Sinha et al., 2015)
344	Sarma cave	Abkhazia (Caucasus)	- 25.37	20.7	344-SAR121	848	SAR-12-1	(Wolf et al., 2024)

Table 7: New entities added to SISALv3.



275 *Figure 3: Trace element ratios and Sr isotope records included in SISALv3 by region. Abbreviations: S. America - South America, N./C. America - North and Central America.*

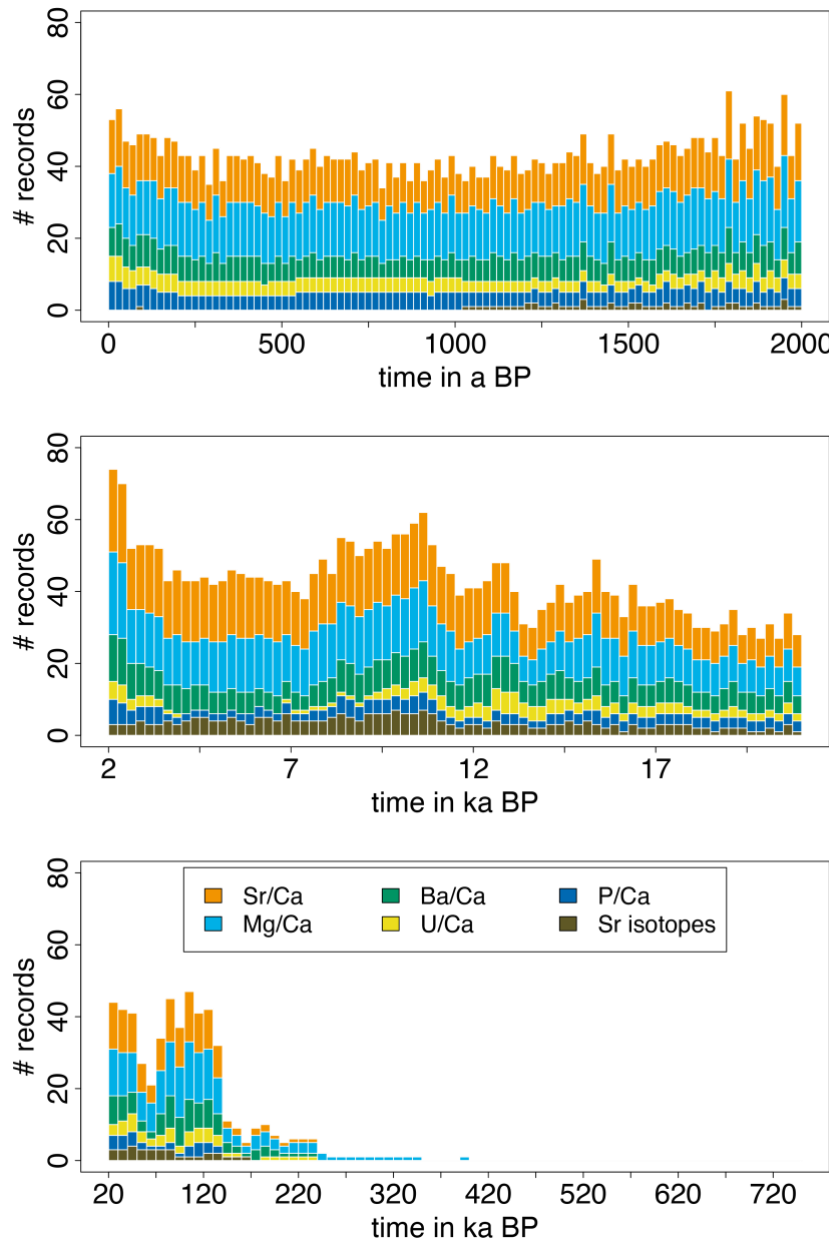


Figure 4: Temporal coverage of the trace element and Sr-isotope records in SISALv3 by region. Entities with multiple trace elements were counted multiple times. Bin sizes: 0-2,000 a (years) BP (top panel) - 20 years; 2,000-21,000 a BP (middle panel) - 250 years; 21,000-750,000 a BP (bottom panel) - 10,000 years.

280

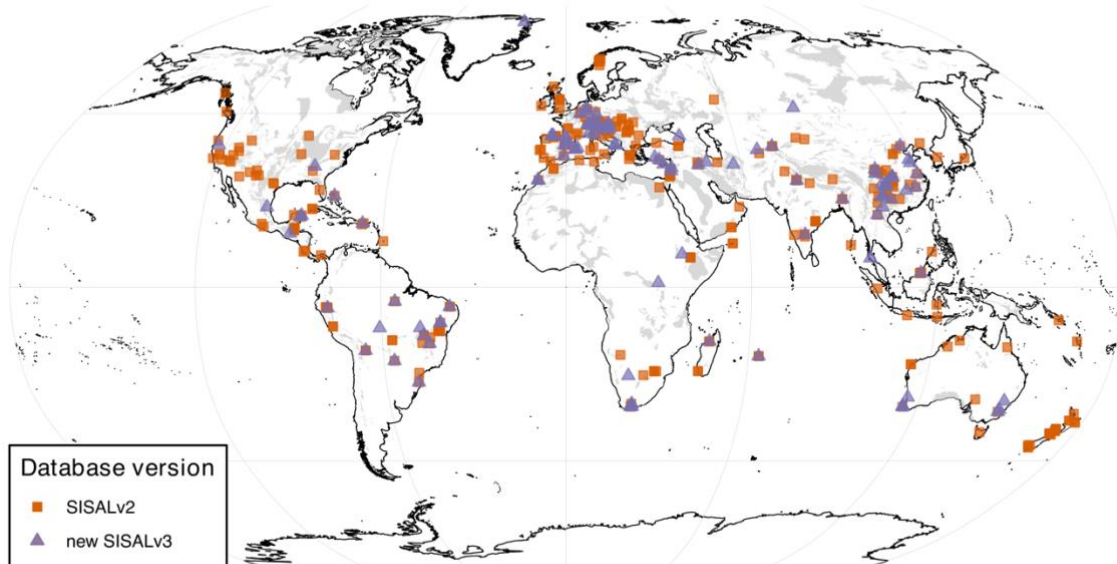


Figure 5: Global map of $\delta^{18}\text{O}$ records included in SISAL v2 and v3. The shaded background shows the global karst distribution extracted from the World Karst Aquifer Map (WOKAM, Goldscheider et al., 2020).

285

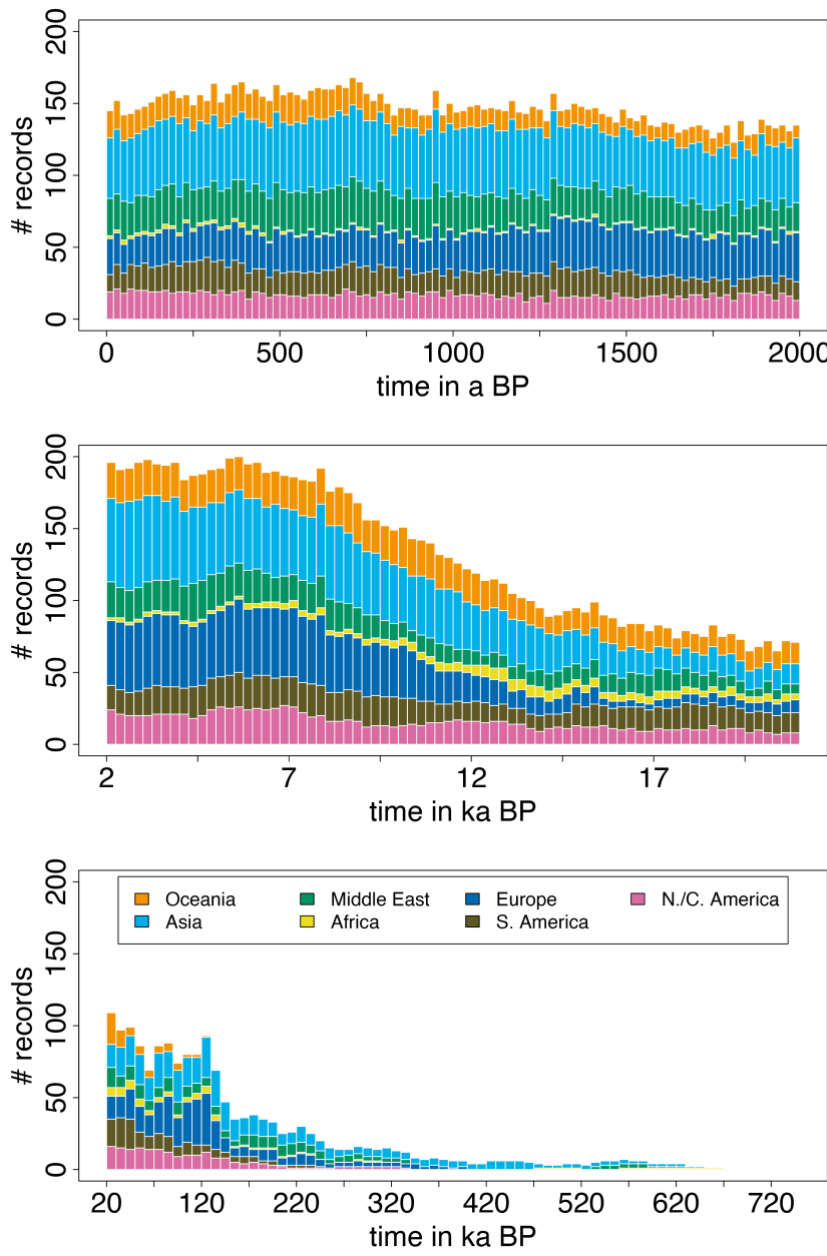
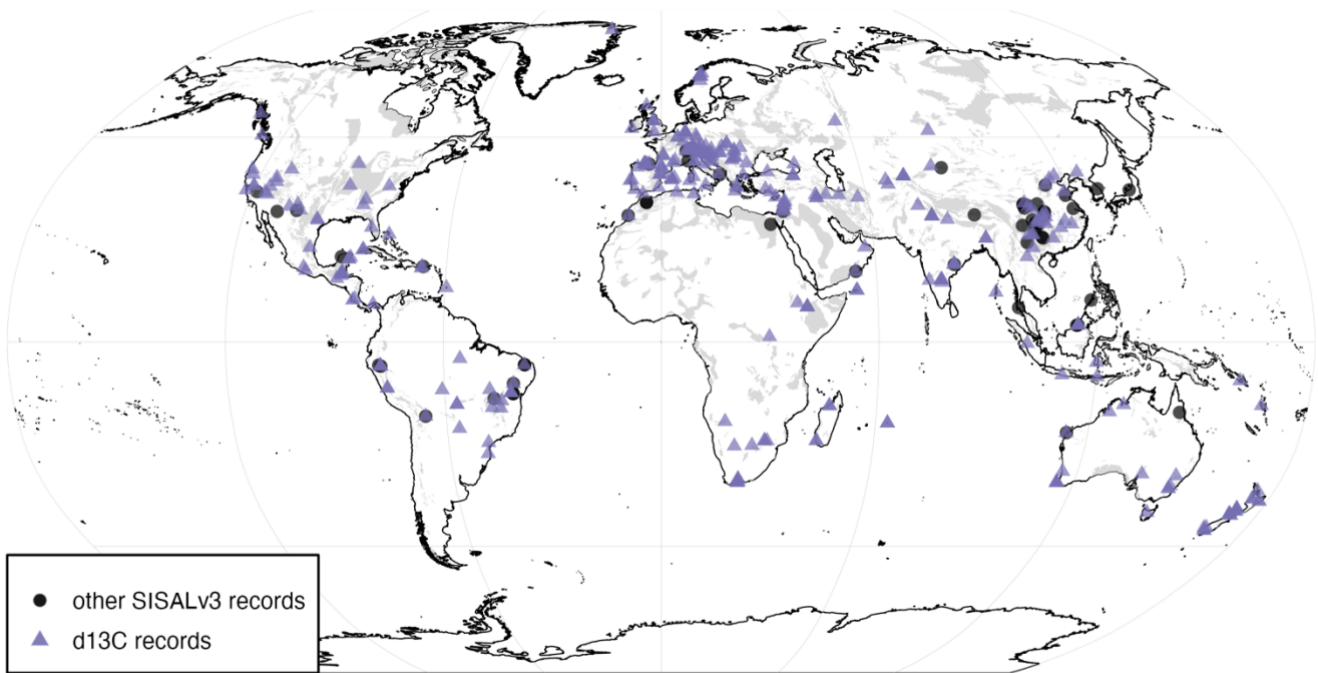


Figure 6: Temporal coverage of the $\delta^{18}\text{O}$ records in SISALv3 by region. Bin sizes: 0-2,000 a BP (top panel) - 20 years; 2,000-21,000 a BP (middle panel) - 250 years; 21,000-750,000 a BP (bottom panel) - 10,000 years.



290 *Figure 7: Map of available $\delta^{13}\text{C}$ records in SISALv3 compared to all records in the database. The shaded background shows the global karst distribution extracted from the World Karst Aquifer Map (WOKAM, Goldscheider et al., 2020).*

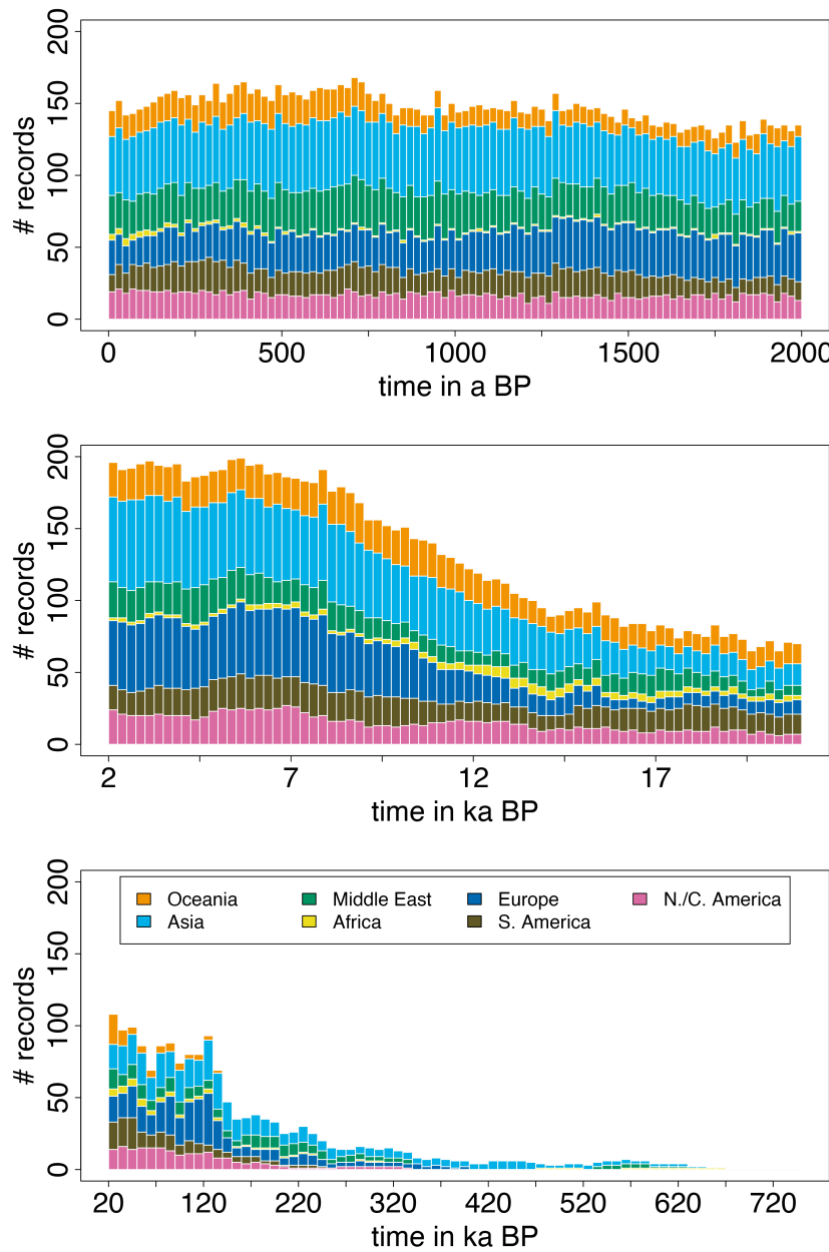


Figure 8: Temporal coverage of the $\delta^{13}\text{C}$ records in SISALv3 by region. Bin sizes: 0-2,000 a BP (top panel) - 20 years; 2,000-

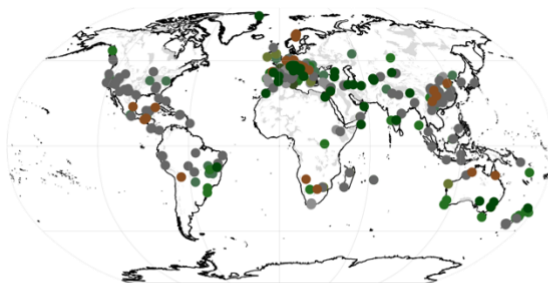
295 21,000 a BP (middle panel) - 250 years; 21,000-750,000 a BP (bottom panel) - 10,000 years.

4.3 Vegetation and land cover metadata

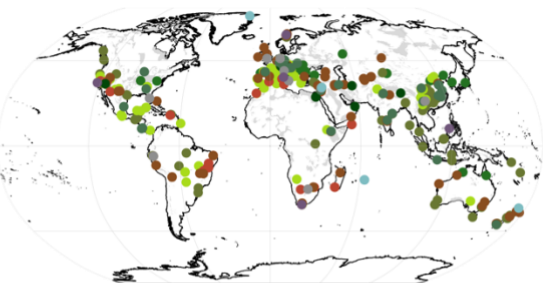
Interpretation of the site-to-site variability in speleothem data sensitive to vegetation changes is facilitated by providing information on *vegetation_type* and *land_use*. The dropdown list for these fields includes options typically used in speleothem publications. Additional information provided by the authors (e.g. species names) has been added to the Notes table.

300 About 40% of the database entries lack the author-reported information on land cover (Figure 9c). Satellite-derived land cover classifications provide information for many more sites (unknown: 1.7%; Figure 9d). Forested sites (evergreen, deciduous, and mixed) comprise ~56.5% (Figure 9d), shrub- and grassland makes up 25.1% and this dataset also denotes sites that are affected by anthropogenic land use (managed vegetation, agriculture, urban), which make up 13%.

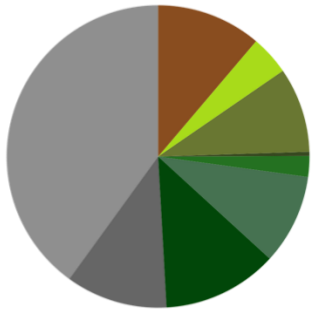
305 (a) Vegetation type location



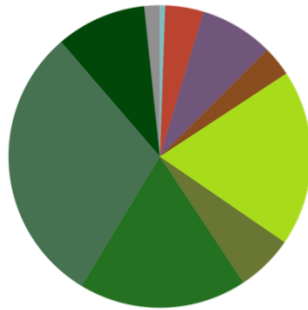
(b) Copernicus LCC location



(c) Vegetation type



(d) Copernicus LCC



A: unknown (40%)
B: other (see notes) (10.9%)
C: deciduous (12.3%)
D: evergreen (9.6%)
E: forest mixed/other (2.2%)
F: moorland (0.4%)
G: shrubs (9.1%)
H: grassland (4.2%)
I: bare / sparse vegetation (11.2%)

A: unknown (1.7%)
B: deciduous (9.6%)
C: evergreen (30%)
D: forest mixed/other (18%)
E: shrubs (6.1%)
F: herbaceous vegetation (18.8%)
G: bare / sparse vegetation (3.2%)
H: cultivated veg. / agriculture (7.9%)
I: urban / built up (4.1%)
J: permanent water bodies (0.6%)

305

310 *Figure 9: (a) – vegetation description from the original publications or provided by authors and (b) – land cover categories extracted from the Copernicus LCC database (Buchhorn et al., 2021, 2020) with a radius of 250 m around the cave sites. (c) - pie chart showing the relative proportions of vegetation types as reported by authors. (d) - pie chart showing the relative proportions of land cover types as extracted from the Copernicus LCC database. Background shading in the map shows the global karst distribution extracted from the World Karst Aquifer Map (WOKAM, (Goldscheider et al., 2020). To allow comparison between the two datasets, the Copernicus LCC vegetation data was grouped into broader categories, e.g., "deciduous" includes all closed and open broad-leaf and needle forest marked as deciduous. The entries in the database are more detailed.*

315 **5 Recommendations for use**

The SISALv3 database is a standardized, quality checked dataset that allows regional to global assessments of spatial and temporal trends in multiple environmental proxies from speleothem records. The addition of trace element data at stable isotope equivalent depths to the database together with machine-readable metadata fields allow examination of hydroclimatic controls on speleothem trace element distribution. Metadata fields, including distance from coast (*latitude*, *longitude*, *elevation*),
320 lithology (*geology*, *wokam*), and land cover (*cover_type*, *cover_thickness*, *vegetation_type*, *land_use*, *copernicus_lcc*), allow identification of the primary controls on trace elements. We recommend using multiple cover fields together, based on the analysis type and scope (e.g., time interval considered) since they provide complementary information. Anthropogenic and natural changes in the cover parameters over time need to be considered, and this applies particularly for the cover fields
325 "*vegetation_type*", "*land_use*" and "*copernicus_lcc*", which in most cases may only be applicable for very recent speleothem growth.

Where trace elements are measured on aliquots of the same powder as stable isotopes, the sample-to-sample variability in depth-time space is minimal. Where samples for stable isotopes and trace elements have been drilled at different times or *in situ* methods have been used for trace element measurements, there may be depth-time variability that may impact results. Extensive metadata on sampling and measurement methods, as well as the original high resolution *in-situ* measurements
330 against depth, are provided in the database and linked repository and should be used to check for such impacts. Measurements may also be sensitive to stalagmite petrography; image scans have been provided in the linked repository so the user can evaluate whether this is important for interpretation of the record.

5.1 Code and data availability

335 The database is available in CSV and SQL format in a repository at <https://doi.org/10.5287/ora-2nanwp4rk> (Kaushal et al., 2024). This dataset is licensed by the rights holder(s) under a Creative Commons Attribution 4.0 International License:
<https://creativecommons.org/licenses/by/4.0/>. Apart from the workbook used to submit data to the SISAL database and the codes for automatic quality checking, the repository contains additional standardisation sheets (coordinate conversion, grams to moles conversion for trace elements, and atomic activity calculator for U-series data). Moreover, the repository contains
340 all submitted cave maps and entity images in separate zip folders, as well as copyright information for the individual images and an entity scan "wishlist" which details best practices for entity scan images. Standardized trace element datafiles are included separately with their metadata (see section 2), and the codes needed to connect and use the database (described in the Readme file).

The codes for standardisation and downsampling of trace element and Sr-isotope records are available at zenodo
345 10.5281/zenodo.8234066 (Skiba, 2023); licensed by the right holder(s) under Creative Commons Attribution 4.0 International).

The database contains both the original age model for individual entities and a standardized age modelling ensemble. The original age model often takes account of site- and sample-specific conditions; the standardized age model ensemble allows for robust assessment of age uncertainties and sensitivity testing (Comas-Bru et al., 2020). All codes for constructing the age model ensembles using linear interpolation, linear regression, Bchron, Bacon, copRa, and StalAge can be found at <https://github.com/paleovar/SISAL.AM> (last access: 23 July 2020; codes licensed by the right holder(s) under a GPL-3 license). These codes are licensed by the right holder(s) under a Creative Commons Attribution 4.0 International. All age model ensembles are available at <https://zenodo.org/records/10726619> (Rehfeld and Bühler, 2024). These codes are licensed by the right holder(s) under a Creative Commons Attribution 4.0 International.

The SISALv3 database, like its predecessors, lists the original references, and users are encouraged to consult original authors for interpretative details. The 'SISAL webApp' (http://geochem.hu/SISAL_webApp; Hatvani et al., 2024) has been updated to provide easy-to-use front-end interface in exploring the latest SISALv3 database. It now allows for querying on various data and metadata fields such as stable isotope records and trace element proxies.

360 **5.2 How to cite the database**

The SISALv3 database is a community driven effort to synthesize, standardize and make speleothem data to the wider paleoclimate community. In agreement with the FAIR principles for scientific data management and stewardship, the database itself should be cited (available at <https://doi.org/10.5287/ora-2nanwp4rk>; Kaushal et al., 2024), together with this publication (and previous version publications). If individual records are extracted from the database, the original publications should also be listed. More details on Terms of Use are provided in the repository (<https://doi.org/10.5287/ora-2nanwp4rk>; Kaushal et al., 2024).

Author contributions

NK, FL and MW designed the new version of the database. KR and JB ran the SISAL standardized age-depth models for new entities. Downsampling of trace element records to stable isotope resolution was performed by VS and MR. Standardization of trace element datafiles was done by YB and NK. Reworking and additions to the metadata fields were done by KB and KA. JGS and NK collected citations, copyright information and license terms for the cave maps and speleothem images. Regional data collection and screening was coordinated by VA, JLB, SC, AC, LE, JH, IGH, ZK, AK, KK, MK, BM, SMA, CN, VFN, CPM, JR, NS, NiS, CT, BHT, SW, AW, HZ. Quality control of the submitted datasets was performed by MW, FL, and NK, with additional code provided by JF. Figures 1 and 2 were created by FL, Figures 3-9 were created by JB. All authors listed as "Data contributors" provided data for this version of the database or helped to complete existing data entries. FL wrote the paper with input from NK, JB, KR, AB, PT, SPH, and all authors contributed to the final version.

Team list

The following SISAL working group members contributed with either data or age-modelling advice to SISALv3: Asfawossen Asrat (Department of Mining and Geological Engineering, Botswana International University of Science and Technology, 380 Private Bag 16, Palapye, Botswana), Charlotte Honiat (Institute of Geology, University of Innsbruck, Innrain 52, Innsbruck, Austria), Dana Felicitas Christine Riehelmann (Institute for Geosciences, Johannes Gutenberg University Mainz, Johann-Joachim-Becher-Weg 21, 55128 Mainz, Germany), Denis Scholz (Institute for Geosciences, Johannes Gutenberg University Mainz, Johann-Joachim-Becher-Weg 21, 55128 Mainz, Germany), Dianbing Liu (School of Geography, Nanjing Normal University, Nanjing 210023, China), Dominik Fleitmann (Department of Environmental Sciences, University of Basel, 385 Bernoullistrasse 32 4056 Basel, Switzerland), Dominik Hennhoefer (Department of Earth Sciences, Khalifa University (SAN Campus), Abu Dhabi, 127788, United Arab Emirates), Ezgi Ünal İmer (Geological Engineering Department, Middle East Technical University, 06800 Çankaya, Ankara, Türkiye), Gina E. Moseley (Institute of Geology, University of Innsbruck, Innrain 52, 390 6020 Innsbruck, Austria), Giselle Utida (Institute of Geosciences, University of São Paulo, 05508-080, Brazil), Hai Cheng (Institute of Global Environmental Change, Xi'an Jiaotong University, China), Helen Green (The University of Melbourne, Parkville VIC 3010, Australia), Hsun-Ming Hu (High-Precision Mass Spectrometry and Environment Change Laboratory (HISPEC), Department of Geosciences, National Taiwan University, Taipei 10617 Taiwan), James Apaéstegui (Instituto Geofísico del Perú, Lima, 15012, Peru), Jan Esper (Department of Geography, Johannes Gutenberg University, Becherweg 21, 395 55099 Mainz, Germany), Jasper A. Wassenburg (1. Center for Climate Physics, Institute for Basic Science, Busan 46241, Republic of Korea 2. Pusan National University, Busan, Republic of Korea), Jeronimo Aviles Olguin (Museo del Desierto. Blvd. Carlos Abedrop Dávila 3745, Nuevo Centro Metropolitano de Saltillo, 25022 Saltillo, Coah. Mexico), Jessica Leigh Oster (Department of Earth and Environmental Sciences, Vanderbilt University, Nashville, TN 37240, USA), Jesús M. Pajón Morejón (National Museum of Natural History of Cuba, Department of Paleogeography and Paleobiology, Obispo 61, Plaza de Armas, Habana Vieja, CP 10 100, La Habana, Cuba), Judit Torner (CRG Marine Geosciences, Facultat de Ciències de la Terra, Universitat de Barcelona, Barcelona, 08028, Spain), Kathleen A Wendt (College of Earth, Ocean, and 400 Atmospheric Sciences, Oregon State University, Corvallis, Oregon 97331, USA), Liangcheng Tan (State Key Laboratory of Loess and Quaternary Geology, Institute of Earth Environment, Chinese Academy of Sciences, Xi'an 710061, China), Lijuan Sha (Institute of Global Environmental Change, Xi'an Jiaotong University, Xi'an 710049, China), Liza Kathleen McDonough (ANSTO, New Illawarra Road, Lucas Heights, NSW 2234, Australia), Maša Surić (Department of Geography, University of Zadar, Ul. dr. F. Tuđmana 24 i, Zadar 23000, Croatia), Matthew J. Jacobson (Division of Agrarian History, Department of 405 Urban and Rural Development, Swedish University of Agricultural Sciences, Uppsala, 756 51, Sweden), Mercè Cisneros (1. GRC Geociències Marines, Departament de Dinàmica de la Terra i de l'Oceà, Facultat de Ciències de la Terra, Universitat de Barcelona. c/ Martí i Franqués s/n, 08028 Barcelona, Spain 2. Centre en Canvi Climàtic, Department de Geografia, Facultat de Turisme i Geografia, Universitat Rovira i Virgili, c/ Joanot Martorell 15, 43480, Vila-seca, Tarragona, Spain), Michael L. Griffiths (Department of Environmental Science, William Paterson University, Wayne NJ, 07739, USA), Michael Weber

410 (Institute for Geosciences, Johannes Gutenberg University Mainz, J.-J.-Becher-Weg 21, 55128 Mainz, Germany), Nick Scroxton (Irish Climate and Analysis Research UnitS (ICARUS), Department of Geography, Maynooth University, Maynooth, Co. Kildare, Ireland), Paul S. Wilcox (Institute of Geology, University of Innsbruck, Innrain 52, 6020 Innsbruck, Austria), R. Lawrence Edwards (Department of Earth and Environmental Sciences, University of Minnesota, Minneapolis, MN 55455, USA), Romina Belli (Proteomics and Mass Spectrometry Core Facility, Department of Cellular, Computational and Integrative
415 Biology (DeCIBIO), University of Trento, Via Sommarive 9, 38123 Trento, Italy), Sebastian F.M. Breitenbach (Department of Geography and Environmental Sciences, Northumbria, Newcastle upon, Tyne NE1 8ST, UK), Shraddha T Band (National Taiwan University, Address: Institute of Oceanography, National Taiwan University No.1, Sec. 4, Roosevelt Road, Taipei 106 ,Taiwan), Simon Dominik Steidle (Institute of Geology, University of Innsbruck, Innrain 52, 6020 Innsbruck, Austria), Stacy Anne Carolin (Department of Earth Sciences, University of Cambridge, Downing Street, Cambridge, CB23 8AD, UK),
420 Vanessa E. Johnston (Karst Research Institute ZRC SAZU, Titov trg 2, 6230 Postojna, Slovenia), Wuhui Duan (1. Key Laboratory of Cenozoic Geology and Environment, Institute of Geology and Geophysics, Chinese Academy of Sciences, Beijing, 100029, China 2. CAS Center for Excellence in Life and Paleoenvironment, Beijing, 100044 China).

Competing interests

425 The authors declare that they have no conflict of interest.

Funding

This study was conducted by SISAL (Speleothem Isotopes Synthesis and Analysis), a working group of the Past Global Changes (PAGES) project. In this framework, we received financial support from the Swiss Academy of Sciences and the
430 Chinese Academy of Sciences. The design and construction of the SISALv3 database were supported financially by a PAGES Data Stewardship Scholarship to F. Lechleitner and N. Kaushal (DSS-108). We also acknowledge funding by PAGES, the Minerva Stiftung (grant 3063000253), and the Institute of Earth Sciences at the Hebrew University Jerusalem (Israel) for supporting the organisation of a workshop to kickstart the initiative.

Acknowledgement

We thank all SISAL members who contributed their data to this project and were available to provide additional information where necessary. We also acknowledge Ana Moreno, Christoph Spötl, and Laura A. Dupont for specific data contributions to

the database. We thank the editorial staff at ESSD and reviewers Ewan Gowan, Christopher Hancock, Sang Chen, and an anonymous referee for their supportive and critical feedback to this manuscript.

440

References

- Allan, M., Delière, A., Verheyden, S., Nicolay, S., Quinif, Y., and Fagel, N.: Evidence for solar influence in a Holocene speleothem record (Père Noël cave, SE Belgium), *Quaternary Science Reviews*, 192, 249–262, <https://doi.org/10.1016/j.quascirev.2018.05.039>, 2018.
- 445 Andrews, J. E., Carolin, S. A., Peckover, E. N., Marca, A., Al-Omari, S., and Rowe, P. J.: Holocene stable isotope record of insolation and rapid climate change in a stalagmite from the Zagros of Iran, *Quaternary Science Reviews*, 241, 106433, <https://doi.org/10.1016/j.quascirev.2020.106433>, 2020.
- 450 Apaéstegui, J., Cruz, F. W., Vuille, M., Fohlmeister, J., Espinoza, J. C., Sifeddine, A., Strikis, N., Guyot, J. L., Ventura, R., Cheng, H., and Edwards, R. L.: Precipitation changes over the eastern Bolivian Andes inferred from speleothem ($\delta^{18}\text{O}$) records for the last 1400 years, *Earth and Planetary Science Letters*, 494, 124–134, <https://doi.org/10.1016/j.epsl.2018.04.048>, 2018.
- Arienzo, M. M., Swart, P. K., Broad, K., Clement, A. C., Pourmand, A., and Kakuk, B.: Multi-proxy evidence of millennial climate variability from multiple Bahamian speleothems, *Quaternary Science Reviews*, 161, 18–29, <https://doi.org/10.1016/j.quascirev.2017.02.004>, 2017.
- 455 Asrat, A., Baker, A., Leng, M. J., Hellstrom, J., Mariethoz, G., Boomer, I., Yu, D., Jex, C. N., and Gunn, J.: Paleoclimate change in Ethiopia around the last interglacial derived from annually-resolved stalagmite evidence, *Quaternary Science Reviews*, 202, 197–210, <https://doi.org/10.1016/j.quascirev.2018.06.016>, 2018.
- Ayalon, A., Bar-Matthews, M., and Sass, E.: Rainfall-recharge relationships within a karstic terrain in the Eastern Mediterranean semi-arid region, Israel: $\delta^{18}\text{O}$ and δD characteristics, *Journal of Hydrology*, 207, 18–31, [https://doi.org/10.1016/S0022-1694\(98\)00119-X](https://doi.org/10.1016/S0022-1694(98)00119-X), 1998.
- 460 Ayalon, A., Bar-Matthews, M., Frumkin, A., and Matthews, A.: Last Glacial warm events on Mount Hermon: the southern extension of the Alpine karst range of the east Mediterranean, *Quaternary Science Reviews*, 59, 43–56, <https://doi.org/10.1016/j.quascirev.2012.10.047>, 2013.
- Azevedo, V., Stríkis, N. M., Santos, R. A., de Souza, J. G., Ampuero, A., Cruz, F. W., de Oliveira, P., Iriarte, J., Stumpf, C. F., Vuille, M., Mendes, V. R., Cheng, H., and Edwards, R. L.: Medieval Climate Variability in the eastern Amazon-Cerrado regions and its archeological implications, *Sci Rep*, 9, 20306, <https://doi.org/10.1038/s41598-019-56852-7>, 2019.
- 465 Azevedo, V., Stríkis, N. M., Novello, V. F., Roland, C. L., Cruz, F. W., Santos, R. V., Vuille, M., Utida, G., De Andrade, F. R. D., Cheng, H., and Edwards, R. L.: Paleo-vegetation seesaw in Brazil since the Late Pleistocene: A multiproxy study of two biomes, *Earth and Planetary Science Letters*, 563, 116880, <https://doi.org/10.1016/j.epsl.2021.116880>, 2021.
- Badertscher, S., Fleitmann, D., Cheng, H., Edwards, R. L., Göktürk, O. M., Zumbühl, A., Leuenberger, M., and Tüysüz, O.: Pleistocene water intrusions from the Mediterranean and Caspian seas into the Black Sea, *Nature Geosci*, 4, 236–239, <https://doi.org/10.1038/ngeo1106>, 2011.

Baker, A., Ito, E., Smart, P. L., and McEwan, R. F.: Elevated and variable values of ^{13}C in speleothems in a British cave system, *Chemical Geology*, 136, 263–270, [https://doi.org/10.1016/S0009-2541\(96\)00129-5](https://doi.org/10.1016/S0009-2541(96)00129-5), 1997.

475 Baker, A., Hartmann, A., Duan, W., Hankin, S., Comas-Bru, L., Cuthbert, M. O., Treble, P. C., Banner, J., Genty, D., Baldini, L. M., Bartolomé, M., Moreno, A., Pérez-Mejías, C., and Werner, M.: Global analysis reveals climatic controls on the oxygen isotope composition of cave drip water, *Nat Commun*, 10, 2984, <https://doi.org/10.1038/s41467-019-11027-w>, 2019.

Baker, A., Mariethoz, G., Comas-Bru, L., Hartmann, A., Frisia, S., Borsato, A., Treble, P. C., and Asrat, A.: The Properties of Annually Laminated Stalagmites-A Global Synthesis, *Reviews of Geophysics*, 59, e2020RG000722, <https://doi.org/10.1029/2020RG000722>, 2021.

480 Baldini, J. U. L., Lechleitner, F. A., Breitenbach, S. F. M., Van Hunen, J., Baldini, L. M., Wynn, P. M., Jamieson, R. A., Ridley, H. E., Baker, A. J., Walczak, I. W., and Fohlmeister, J.: Detecting and quantifying palaeoseasonality in stalagmites using geochemical and modelling approaches, *Quaternary Science Reviews*, 254, 106784, <https://doi.org/10.1016/j.quascirev.2020.106784>, 2021.

485 Baldini, L. M., Baldini, J. U. L., McDermott, F., Arias, P., Cueto, M., Fairchild, I. J., Hoffmann, D. L., Matthey, D. P., Müller, W., Nita, D. C., Ontañón, R., Garcíá-Moncó, C., and Richards, D. A.: North Iberian temperature and rainfall seasonality over the Younger Dryas and Holocene, *Quaternary Science Reviews*, 226, 105998, <https://doi.org/10.1016/j.quascirev.2019.105998>, 2019.

490 Band, S. T., Yadava, M. G., Kaushal, N., Midhun, M., Thirumalai, K., Francis, T., Laskar, A., Ramesh, R., Henderson, G. M., and Narayana, A. C.: Southern hemisphere forced millennial scale Indian summer monsoon variability during the late Pleistocene, *Sci Rep*, 12, 10136, <https://doi.org/10.1038/s41598-022-14010-6>, 2022.

Bar-Matthews, M., Ayalon, A., Gilmour, M., Matthews, A., and Hawkesworth, C. J.: Sea-land oxygen isotopic relationships from planktonic foraminifera and speleothems in the Eastern Mediterranean region and their implication for paleorainfall during interglacial intervals, *Geochimica et Cosmochimica Acta*, 67, 3181–3199, [https://doi.org/10.1016/S0016-7037\(02\)01031-1](https://doi.org/10.1016/S0016-7037(02)01031-1), 2003.

495 Bar-Matthews, M., Marean, C. W., Jacobs, Z., Karkanas, P., Fisher, E. C., Herries, A. I. R., Brown, K., Williams, H. M., Bernatchez, J., Ayalon, A., and Nilssen, P. J.: A high resolution and continuous isotopic speleothem record of paleoclimate and paleoenvironment from 90 to 53 ka from Pinnacle Point on the south coast of South Africa, *Quaternary Science Reviews*, 29, 2131–2145, <https://doi.org/10.1016/j.quascirev.2010.05.009>, 2010.

500 Belli, R., Frisia, S., Borsato, A., Drysdale, R., Hellstrom, J., Zhao, J. X., and Spötl, C.: Regional climate variability and ecosystem responses to the last deglaciation in the northern hemisphere from stable isotope data and calcite fabrics in two northern Adriatic stalagmites, *Quaternary Science Reviews*, 72, 146–158, <https://doi.org/10.1016/j.quascirev.2013.04.014>, 2013.

505 Belli, R., Borsato, A., Frisia, S., Drysdale, R., Maas, R., and Greig, A.: Investigating the hydrological significance of stalagmite geochemistry (Mg, Sr) using Sr isotope and particulate element records across the Late Glacial-to-Holocene transition, *Geochimica et Cosmochimica Acta*, 199, 247–263, <https://doi.org/10.1016/j.gca.2016.10.024>, 2017.

Bernal-Wormull, J. L., Moreno, A., Pérez-Mejías, C., Bartolomé, M., Aranburu, A., Arriolabengoa, M., Iriarte, E., Cacho, I., Spötl, C., Edwards, R. L., and Cheng, H.: Immediate temperature response in northern Iberia to last deglacial changes in the North Atlantic, *Geology*, 49, 999–1003, <https://doi.org/10.1130/G48660.1>, 2021.

- 510 Borsato, A., Frisia, S., Fairchild, I. J., Somogyi, A., and Susini, J.: Trace element distribution in annual stalagmite laminae mapped by micrometer-resolution X-ray fluorescence: Implications for incorporation of environmentally significant species, *Geochimica et Cosmochimica Acta*, 71, 1494–1512, <https://doi.org/10.1016/j.gca.2006.12.016>, 2007.
- Braun, K., Nehme, C., Pickering, R., Rogerson, M., and Scropton, N.: A Window into Africa's Past Hydroclimates: The SISAL_v1 Database Contribution, *Quaternary*, 2, 4, <https://doi.org/10.3390/quat2010004>, 2019a.
- 515 Braun, K., Bar-Matthews, M., Matthews, A., Ayalon, A., Cowling, R. M., Karkanas, P., Fisher, E. C., Dyez, K., Zilberman, T., and Marean, C. W.: Late Pleistocene records of speleothem stable isotopic compositions from Pinnacle Point on the South African south coast, *Quaternary Research*, 91, 265–288, <https://doi.org/10.1017/qua.2018.61>, 2019b.
- Braun, K., Bar-Matthews, M., Matthews, A., Ayalon, A., Zilberman, T., Cowling, R. M., Fisher, E. C., Herries, A. I. R., Brink, J. S., and Marean, C. W.: Comparison of climate and environment on the edge of the Palaeo-Agulhas Plain to the Little Karoo (South Africa) in Marine Isotope Stages 5–3 as indicated by speleothems, *Quaternary Science Reviews*, 235, 105803, <https://doi.org/10.1016/j.quascirev.2019.06.025>, 2020.
- 520 Buchhorn, M., Lesiv, M., Tsedbazar, N.-E., Herold, M., Bertels, L., and Smets, B.: Copernicus Global Land Cover Layers—Collection 2, *Remote Sensing*, 12, 1044, <https://doi.org/10.3390/rs12061044>, 2020.
- Buchhorn, M., Smets, B., Bertels, L., Roo, B. D., Lesiv, M., Tsedbazar, N.-E., Li, L., and Tarko, A.: Copernicus Global Land Service: Land Cover 100m: version 3 Globe 2015-2019: Product User Manual, Zenodo, <https://doi.org/10.5281/zenodo.4723921>, 2021.
- 525 Buckingham, F. L., Carolin, S. A., Partin, J. W., Adkins, J. F., Cobb, K. M., Day, C. C., Ding, Q., He, C., Liu, Z., Otto-Bliesner, B., Roberts, W. H. G., Lejau, S., and Malang, J.: Termination 1 Millennial-Scale Rainfall Events Over the Sunda Shelf, *Geophysical Research Letters*, 49, e2021GL096937, <https://doi.org/10.1029/2021GL096937>, 2022.
- Budsky, A., Scholz, D., Wassenburg, J. A., Mertz-Kraus, R., Spötl, C., Riechelmann, D. F., Gibert, L., Jochum, K. P., and 530 Andreæ, M. O.: Speleothem $\delta^{13}\text{C}$ record suggests enhanced spring/summer drought in south-eastern Spain between 9.7 and 7.8 ka – A circum-Western Mediterranean anomaly?, *The Holocene*, 29, 1113–1133, <https://doi.org/10.1177/0959683619838021>, 2019.
- Bühler, J. C., Axelsson, J., Lechleitner, F. A., Fohlmeister, J., LeGrande, A. N., Midhun, M., Sjolte, J., Werner, M., Yoshimura, K., and Rehfeld, K.: Investigating stable oxygen and carbon isotopic variability in speleothem records over the last millennium 535 using multiple isotope-enabled climate models, *Climate of the Past*, 18, 1625–1654, <https://doi.org/10.5194/cp-18-1625-2022>, 2022.
- Burstyn, Y., Martrat, B., Lopez, J. F., Iriarte, E., Jacobson, M. J., Lone, M. A., and Deininger, M.: Speleothems from the Middle East: An Example of Water Limited Environments in the SISAL Database, *Quaternary*, 2, 16, <https://doi.org/10.3390/quat2020016>, 2019.
- 540 Carolin, S. A., Ersek, V., Roberts, W. H. G., Walker, R. T., and Henderson, G. M.: Drying in the Middle East During Northern Hemisphere Cold Events of the Early Glacial Period, *Geophysical Research Letters*, 46, 14003–14010, <https://doi.org/10.1029/2019GL084365>, 2019a.
- Carolin, S. A., Walker, R. T., Day, C. C., Ersek, V., Sloan, R. A., Dee, M. W., Talebian, M., and Henderson, G. M.: Precise 545 timing of abrupt increase in dust activity in the Middle East coincident with 4.2 ka social change, *Proceedings of the National Academy of Sciences*, 116, 67–72, <https://doi.org/10.1073/pnas.1808103115>, 2019b.

Chawchai, S., Tan, L., Löwemark, L., Wang, H.-C., Yu, T.-L., Chung, Y.-C., Mii, H.-S., Liu, G., Blaauw, M., Gong, S.-Y., Wohlfarth, B., and Shen, C.-C.: Hydroclimate variability of central Indo-Pacific region during the Holocene, Quaternary Science Reviews, 253, 106779, <https://doi.org/10.1016/j.quascirev.2020.106779>, 2021.

550 Chen, C., Yuan, D., Cheng, H., Yu, T., Shen, C., Edwards, R. L., Wu, Y., Xiao, S., Zhang, J., Wang, T., Huang, R., Liu, Z., Li, T., and Li, J.: Human activity and climate change triggered the expansion of rocky desertification in the karst areas of Southwestern China, Sci. China Earth Sci., 64, 1761–1773, <https://doi.org/10.1007/s11430-020-9760-7>, 2021.

Cheng, H., Edwards, R. L., Broecker, W. S., Denton, G. H., Kong, X., Wang, Y., Zhang, R., and Wang, X.: Ice age terminations., Science (New York, N.Y.), 326, 248–252, <https://doi.org/10.1126/science.1177840>, 2009a.

555 Cheng, H., Fleitmann, D., Edwards, R. L., Wang, X., Cruz, F. W., Auler, A. S., Mangini, A., Wang, Y., Kong, X., Burns, S. J., and Matter, A.: Timing and structure of the 8.2 kyr B.P. event inferred from $\delta^{18}\text{O}$ records of stalagmites from China, Oman, and Brazil, Geology, 37, 1007–1010, <https://doi.org/10.1130/G30126A.1>, 2009b.

Cheng, H., Sinha, A., Cruz, F. W., Wang, X., Edwards, R. L., Horta, F. M., Ribas, C. C., Vuille, M., Stott, L. D., and Auler, A. S.: Climate change in Amazonia and biodiversity, Nature Communications, 4, <https://doi.org/10.1038/ncomms2415>, 2013.

560 Cheng, H., Edwards, R. L., Sinha, A., Spötl, C., Yi, L., Chen, S., Kelly, M., Kathayat, G., Wang, X., Li, X., Kong, X., Wang, Y., Ning, Y., and Zhang, H.: The Asian monsoon over the past 640,000 years and ice age terminations, Nature, 534, 640–646, <https://doi.org/10.1038/nature18591>, 2016.

Cheng, H., Springer, G. S., Sinha, A., Hardt, B. F., Yi, L., Li, H., Tian, Y., Li, X., Rowe, H. D., Kathayat, G., Ning, Y., and Edwards, R. L.: Eastern North American climate in phase with fall insolation throughout the last three glacial-interglacial cycles, Earth and Planetary Science Letters, 522, 125–134, <https://doi.org/10.1016/j.epsl.2019.06.029>, 2019.

565 Cheng, H., Xu, Y., Dong, X., Zhao, J., Li, H., Baker, J., Sinha, A., Spötl, C., Zhang, H., Du, W., Zong, B., Jia, X., Kathayat, G., Liu, D., Cai, Y., Wang, X., Strikis, N. M., Cruz, F. W., Auler, A. S., Gupta, A. K., Singh, R. K., Jaglan, S., Dutt, S., Liu, Z., and Edwards, R. L.: Onset and termination of Heinrich Stadial 4 and the underlying climate dynamics, Commun Earth Environ, 2, 1–11, <https://doi.org/10.1038/s43247-021-00304-6>, 2021.

570 Cisneros, M., Cacho, I., Moreno, A., Stoll, H., Torner, J., Català, A., Edwards, R. L., Cheng, H., and Fornós, J. J.: Hydroclimate variability during the last 2700 years based on stalagmite multi-proxy records in the central-western Mediterranean, Quaternary Science Reviews, 269, 107137, <https://doi.org/10.1016/j.quascirev.2021.107137>, 2021.

Columbu, A., Drysdale, R., Hellstrom, J., Woodhead, J., Cheng, H., Hua, Q., Zhao, J., Montagna, P., Pons-Branchu, E., and Edwards, R. L.: U-Th and radiocarbon dating of calcite speleothems from gypsum caves (Emilia Romagna, North Italy), Quaternary Geochronology, 52, 51–62, <https://doi.org/10.1016/j.quageo.2019.04.002>, 2019.

575 Columbu, A., Chiarini, V., Spötl, C., Benazzi, S., Hellstrom, J., Cheng, H., and De Waele, J.: Speleothem record attests to stable environmental conditions during Neanderthal-modern human turnover in southern Italy, Nat Ecol Evol, 4, 1188–1195, <https://doi.org/10.1038/s41559-020-1243-1>, 2020.

580 Columbu, A., Spötl, C., Fohlmeister, J., Hu, H.-M., Chiarini, V., Hellstrom, J., Cheng, H., Shen, C.-C., and De Waele, J.: Central Mediterranean rainfall varied with high northern latitude temperatures during the last deglaciation, Commun Earth Environ, 3, 1–9, <https://doi.org/10.1038/s43247-022-00509-3>, 2022.

Comas-Bru, L. and Harrison, S. P.: SISAL: Bringing added value to speleothem research, Quaternary, 2, <https://doi.org/10.3390/quat2010007>, 2019.

Comas-Bru, L., Deininger, M., Harrison, S., Bar-Matthews, M., Baker, A., Duan, W., and Stríkis, N.: Speleothem synthesis and analysis working group, PAGES Mag, 25, 129–129, <https://doi.org/10.22498/pages.25.2.129>, 2017.

585 Comas-Bru, L., Harrison, S. P., Werner, M., Rehfeld, K., Scroxton, N., Veiga-Pires, C., Ahmad, S. M., Brahim, Y. A., Mozhdehi, S. A., Arienzo, M., Atsawawaranunt, K., Baker, A., Braun, K., Breitenbach, S., Burstyn, Y., Chawchai, S., Columbu, A., Deininger, M., Demény, A., Dixon, B., Hatvani, I. G., Hu, J., Kaushal, N., Kern, Z., Labuhn, I., Lachniet, M. S., Lechleitner, F. A., Lorrey, A., Markowska, M., Nehme, C., Novello, V. F., Oster, J., Pérez-Mejías, C., Pickering, R., Sekhon, N., Wang, X., Warken, S., Atkinson, T., Ayalon, A., Baldini, J., Bar-Matthews, M., Bernal, J. P., Boch, R., Borsato, A., Boyd, M., Brierley, C., Cai, Y., Carolin, S., Cheng, H., Constantin, S., Couchoud, I., Cruz, F., Denniston, R., Dragusin, V., Duan, W., Ersek, V., Finné, M., Fleitmann, D., Fohlmeister, J., Frappier, A., Genty, D., Holzkämper, S., Hopley, P., Johnston, V., Kathayat, G., Keenan-Jones, D., Koltai, G., Li, T.-Y., Lone, M. A., Luetscher, M., Mattey, D., Moreno, A., Moseley, G., Psomiadis, D., Ruan, J., Scholz, D., Sha, L., Smith, A. C., Strikis, N., Treble, P., Ünal-Imer, E., Vaks, A., Vansteenberge, S., Voarintsoa, N. R. G., Wong, C., Wortham, B., Wurtzel, J., and Zhang, H.: Evaluating model outputs using integrated global speleothem records of climate change since the last glacial, Climate of the Past, 15, <https://doi.org/10.5194/cp-15-1557-2019>, 2019.

590 Comas-Bru, L., Rehfeld, K., Roesch, C., Amirnezhad-Mozhdehi, S., Harrison, S. P., Atsawawaranunt, K., Ahmad, S. M., Ait Brahim, Y., Baker, A., Bosomworth, M., Breitenbach, S. F. M., Burstyn, Y., Columbu, A., Deininger, M., Demény, A., Dixon, B., Fohlmeister, J., Hatvani, I. G., Hu, J., Kaushal, N., Kern, Z., Labuhn, I., Lechleitner, F. A., Lorrey, A., Martrat, B., Novello, V. F., Oster, J., Pérez-Mejías, C., Scholz, D., Scroxton, N., Sinha, N., Ward, B. M., Warken, S., Zhang, H., and Working Group Members, S.: SISALv2: A comprehensive speleothem isotope database with multiple age-depth models, Earth System Science Data, 12, 2579–2606, <https://doi.org/10.5194/essd-2020-39>, 2020.

600 Covington, M. D. and Perne, M.: Consider a cylindrical cave: A physicist's view of cave and karst science, Acta Carsologica, 44, <https://doi.org/10.3986/ac.v44i3.1925>, 2015.

605 Cruz, F. W., Burns, S. J., Jercinovic, M., Karmann, I., Sharp, W. D., and Vuille, M.: Evidence of rainfall variations in Southern Brazil from trace element ratios (Mg/Ca and Sr/Ca) in a Late Pleistocene stalagmite, Geochimica et Cosmochimica Acta, 71, 2250–2263, <https://doi.org/10.1016/j.gca.2007.02.005>, 2007.

610 Day, C. C. and Henderson, G. M.: Controls on trace-element partitioning in cave-analogue calcite, Geochimica et Cosmochimica Acta, 120, 612–627, <https://doi.org/10.1016/j.gca.2013.05.044>, 2013.

615 Deininger, M., Ward, B. M., Novello, V. F., and Cruz, F. W.: Late Quaternary Variations in the South American Monsoon System as Inferred by Speleothems—New Perspectives Using the SISAL Database, Quaternary, 2, 6, <https://doi.org/10.3390/quat2010006>, 2019.

Della Libera, M. E., Novello, V. F., Cruz, F. W., Orrison, R., Vuille, M., Maezumi, S. Y., de Souza, J., Cauhy, J., Campos, J. L. P. S., Ampuero, A., Utida, G., Stríkis, N. M., Stumpf, C. F., Azevedo, V., Zhang, H., Edwards, R. L., and Cheng, H.: Paleoclimatic and paleoenvironmental changes in Amazonian lowlands over the last three millennia, Quaternary Science Reviews, 279, 107383, <https://doi.org/10.1016/j.quascirev.2022.107383>, 2022.

620 Dorale, J. A., Edwards, L. R., Ito, E., and Gonzalez, L. A.: Climate and Vegetation History of the Midcontinent from 75 to 25 ka: A Speleothem Record from Crevice Cave, Missouri, USA | Science, Science (New York, N.Y.), 282, 1871–1874, 1998.

Drysdale, R., Couchoud, I., Zanchetta, G., Isola, I., Regattieri, E., Hellstrom, J., Govin, A., Tzedakis, P. C., Ireland, T., Corrick, E., Greig, A., Wong, H., Piccini, L., Holden, P., and Woodhead, J.: Magnesium in subaqueous speleothems as a potential palaeotemperature proxy, Nat Commun, 11, 5027, <https://doi.org/10.1038/s41467-020-18083-7>, 2020.

Duan, W., Cheng, H., Tan, M., Li, X., and Lawrence Edwards, R.: Timing and structure of Termination II in north China constrained by a precisely dated stalagmite record, *Earth and Planetary Science Letters*, 512, 1–7, <https://doi.org/10.1016/j.epsl.2019.01.043>, 2019.

625 Duan, W., Wang, X., Tan, M., Cui, L., Wang, X., and Xiao, Z.: Variable Phase Relationship Between Monsoon and Temperature in East Asia During Termination II Revealed by Oxygen and Clumped Isotopes of a Northern Chinese Stalagmite, *Geophysical Research Letters*, 49, e2022GL098296, <https://doi.org/10.1029/2022GL098296>, 2022.

630 Dupont, L. A., Railsback, L. B., Liang, F., Brook, G. A., Cheng, H., and Edwards, R. L.: Episodic deposition of stalagmites in the northeastern Democratic Republic of the Congo suggests Equatorial Humid Periods during insolation maxima, *Quaternary Science Reviews*, 286, 107552, <https://doi.org/10.1016/j.quascirev.2022.107552>, 2022.

Fairchild, I. J. and Treble, P. C.: Trace elements in speleothems as recorders of environmental change, *Quaternary Science Reviews*, 28, 449–468, <https://doi.org/10.1016/j.quascirev.2008.11.007>, 2009.

635 Fairchild, I. J., Borsato, A., Tooth, A. F., Frisia, S., Hawkesworth, C. J., Huang, Y., McDermott, F., and Spiro, B.: Controls on trace element (Sr-Mg) compositions of carbonate cave waters: implications for speleothem climatic records, *Chemical Geology*, 166, 255–269, 2000.

Faraji, M., Borsato, A., Frisia, S., Hartland, A., Hellstrom, J. C., and Greig, A.: High-resolution reconstruction of infiltration in the Southern Cook Islands based on trace elements in speleothems, *Quaternary Research*, 1–21, <https://doi.org/10.1017/qua.2023.51>, 2023.

640 Finestone, E. M., Breeze, P. S., Breitenbach, S. F. M., Drake, N., Bergmann, L., Maksudov, F., Muhammadiyev, A., Scott, P., Cai, Y., Khatsenovich, A. M., Rybin, E. P., Nehrke, G., Boivin, N., and Petraglia, M.: Paleolithic occupation of arid Central Asia in the Middle Pleistocene, *PLOS ONE*, 17, e0273984, <https://doi.org/10.1371/journal.pone.0273984>, 2022.

Flohr, P., Fleitmann, D., Zorita, E., Sadekov, A., Cheng, H., Bosomworth, M., Edwards, L., Matthews, W., and Matthews, R.: Late Holocene droughts in the Fertile Crescent recorded in a speleothem from northern Iraq, *Geophysical Research Letters*, 44, 1528–1536, <https://doi.org/10.1002/2016GL071786>, 2017.

645 Fohlmeister, J., Vollweiler, N., Spötl, C., and Mangini, A.: COMNISPA II: Update of a mid-European isotope climate record, 11 ka to present, *The Holocene*, 23, 749–754, <https://doi.org/10.1177/0959683612465446>, 2013.

Fohlmeister, J., Voarintsoa, N. R. G., Lechleitner, F. A., Boyd, M., Brandstätter, S., Jacobson, M. J., and Oster, J. L.: Main controls on the stable carbon isotope composition of speleothems, *Geochimica et Cosmochimica Acta*, 279, 67–87, <https://doi.org/10.1016/j.gca.2020.03.042>, 2020.

650 Frumkin, A., Ford, D. C., and Schwarcz, H. P.: Continental Oxygen Isotopic Record of the Last 170,000 Years in Jerusalem, *Quaternary Research*, 51, 317–327, <https://doi.org/10.1006/qres.1998.2031>, 1999.

Genty, D., Blamart, D., Ouahdi, R., Gilmour, M., Baker, A., Jouzel, J., and Van-Exter, S.: Precise dating of Dansgaard-Oeschger climate oscillations in western Europe from stalagmite data., *Nature*, 421, 833–837, <https://doi.org/10.1038/nature01391>, 2003.

655 Genty, D., Blamart, D., Ghaleb, B., Plagnes, V., Causse, C., Bakalowicz, M., Zouari, K., Chkir, N., Hellstrom, J., Wainer, K., and Bourges, F.: Timing and dynamics of the last deglaciation from European and North African $\delta^{13}\text{C}$ stalagmite profiles - Comparison with Chinese and South Hemisphere stalagmites, *Quaternary Science Reviews*, 25, 2118–2142, <https://doi.org/10.1016/j.quascirev.2006.01.030>, 2006.

- 660 Goede, A., McCulloch, M., McDermott, F., and Hawkesworth, C.: Aeolian contribution to strontium and strontium isotope variations in a tasmanian speleothem, *Chemical Geology*, [https://doi.org/10.1016/S0009-2541\(98\)00035-7](https://doi.org/10.1016/S0009-2541(98)00035-7), 1998.
- Goldscheider, N., Chen, Z., Auler, A. S., Bakalowicz, M., Broda, S., Drew, D., Hartmann, J., Jiang, G., Moosdorf, N., Stevanovic, Z., and Veni, G.: Global distribution of carbonate rocks and karst water resources, *Hydrogeol J*, 28, 1661–1677, <https://doi.org/10.1007/s10040-020-02139-5>, 2020.
- 665 Green, H., Pickering, R., Drysdale, R., Johnson, B. C., Hellstrom, J., and Wallace, M.: Evidence for global teleconnections in a late Pleistocene speleothem record of water balance and vegetation change at Sudwala Cave, South Africa, *Quaternary Science Reviews*, 110, 114–130, <https://doi.org/10.1016/j.quascirev.2014.11.016>, 2015.
- Griffiths, M. L., Johnson, K. R., Pausata, F. S. R., White, J. C., Henderson, G. M., Wood, C. T., Yang, H., Ersek, V., Conrad, C., and Sekhon, N.: End of Green Sahara amplified mid- to late Holocene megadroughts in mainland Southeast Asia, *Nat Commun*, 11, 4204, <https://doi.org/10.1038/s41467-020-17927-6>, 2020.
- 670 Hatvani, I. G., Kern, Z., Tanos, P., Wilhelm, M., Lechleitner, F. A., and Kaushal, N.: The SISAL webApp: exploring the speleothem climate and environmental archives of the world, *Quaternary Research*, 1–7, <https://doi.org/10.1017/qua.2023.39>, 2024.
- Henderson, G. M.: Caving in to new chronologies., *Science*, 313, 620–622, <https://doi.org/10.1126/science.1128980>, 2006.
- 675 Honiat, C., Festi, D., Wilcox, P. S., Edwards, R. L., Cheng, H., and Spötl, C.: Early Last Interglacial environmental changes recorded by speleothems from Katerloch (south-east Austria), *Journal of Quaternary Science*, 37, 664–676, <https://doi.org/10.1002/jqs.3398>, 2022.
- Hu, C., Henderson, G. M., Huang, J., Xie, S., Sun, Y., and Johnson, K. R.: Quantification of Holocene Asian monsoon rainfall from spatially separated cave records, *Earth and Planetary Science Letters*, 266, 221–232, <https://doi.org/10.1016/j.epsl.2007.10.015>, 2008.
- 680 Hu, H.-M., Michel, V., Valensi, P., Mii, H.-S., Starnini, E., Zunino, M., and Shen, C.-C.: Stalagmite-Inferred Climate in the Western Mediterranean during the Roman Warm Period, *Climate*, 10, 93, <https://doi.org/10.3390/cli10070093>, 2022.
- Huang, Y., Fairchild, I. J., Borsato, A., Frisia, S., Cassidy, N. J., McDermott, F., and Hawkesworth, C. J.: Seasonal variations in Sr, Mg and P in modern speleothems (Grotta di Ernesto, Italy), *Chemical Geology*, 175, 429–448, [https://doi.org/10.1016/S0009-2541\(00\)00337-5](https://doi.org/10.1016/S0009-2541(00)00337-5), 2001.
- 685 Jacobson, M. J., Flohr, P., Gascoigne, A., Leng, M. J., Sadekov, A., Cheng, H., Edwards, R. L., Tüysüz, O., and Fleitmann, D.: Heterogenous Late Holocene Climate in the Eastern Mediterranean—The Kocain Cave Record From SW Turkey, *Geophysical Research Letters*, 48, e2021GL094733, <https://doi.org/10.1029/2021GL094733>, 2021.
- Jamieson, R. A., Baldini, J. U. L., Brett, M. J., Taylor, J., Ridley, H. E., Ottley, C. J., Pruffer, K. M., Wassenburg, J. A., Scholz, D., and Breitenbach, S. F. M.: Intra- and inter-annual uranium concentration variability in a Belizean stalagmite controlled by prior aragonite precipitation : A new tool for reconstructing hydro-climate using aragonitic speleothems, *Geochimica et Cosmochimica Acta*, <https://doi.org/10.1016/j.gca.2016.06.037>, 2016.
- Johnson, K. R., Hu, C., Belshaw, N. S., and Henderson, G. M.: Seasonal trace-element and stable-isotope variations in a Chinese speleothem: The potential for high-resolution paleomonsoon reconstruction, *Earth and Planetary Science Letters*, 244, 394–407, <https://doi.org/10.1016/j.epsl.2006.01.064>, 2006.

- 695 Johnston, V. E., Borsato, A., Frisia, S., Spötl, C., Hellstrom, J. C., Cheng, H., and Edwards, R. L.: Last interglacial hydroclimate in the Italian Prealps reconstructed from speleothem multi-proxy records (Bigonda Cave, NE Italy), Quaternary Science Reviews, 272, 107243, <https://doi.org/10.1016/j.quascirev.2021.107243>, 2021.
- Kathayat, G., Cheng, H., Sinha, A., Spötl, C., Edwards, R. L., Zhang, H., Li, X., Yi, L., Ning, Y., Cai, Y., Lui Lui, W., and Breitenbach, S. F. M.: Indian monsoon variability on millennial-orbital timescales, Scientific Reports, 6, 700 <https://doi.org/10.1038/srep24374>, 2016.
- Kaushal, N., Breitenbach, S. F. M., Lechleitner, F. A., Sinha, A., Tewari, V. C., Ahmad, S. M., Berkelhammer, M., Band, S., Yadava, M., Ramesh, R., and Henderson, G. M.: The Indian Summer Monsoon from a Speleothem $\delta^{18}\text{O}$ Perspective—A Review, Quaternary, 1, 29, <https://doi.org/10.3390/quat1030029>, 2018.
- Kaushal, N., Lechleitner, F. A., Wilhelm, M., and SISAL Working Group Members: SISALv3: Speleothem Isotopes Synthesis and AnaLysis database version 3.0, <https://doi.org/10.5287/ora-2nanwp4rk>, 2024.
- Kelly, M. J., Edwards, R. L., Cheng, H., Yuan, D., Cai, Y., Zhang, M., Lin, Y., and An, Z.: High resolution characterization of the Asian Monsoon between 146,000 and 99,000 years B.P. from Dongge Cave, China and global correlation of events surrounding Termination II, Palaeogeography, Palaeoclimatology, Palaeoecology, 236, 20–38, <https://doi.org/10.1016/j.palaeo.2005.11.042>, 2006.
- 710 Kern, Z., Demény, A., Perșoiu, A., and Hatvani, I. G.: Speleothem Records from the Eastern Part of Europe and Turkey—Discussion on Stable Oxygen and Carbon Isotopes, Quaternary, 2, 31, <https://doi.org/10.3390/quat2030031>, 2019.
- Koltai, G., Spötl, C., Shen, C.-C., Wu, C.-C., Rao, Z., Palcsu, L., Kele, S., Surányi, G., and Bárány-Kevei, I.: A penultimate glacial climate record from southern Hungary, Journal of Quaternary Science, 32, 946–956, <https://doi.org/10.1002/jqs.2968>, 2017.
- 715 Lachniet, M. S., Denniston, R. F., Asmerom, Y., and Polyak, V. J.: Orbital control of western North America atmospheric circulation and climate over two glacial cycles, Nat Commun, 5, 3805, <https://doi.org/10.1038/ncomms4805>, 2014.
- Lechleitner, F. A., Amirnezhad-Mozhdehi, S., Columbu, A., Comas-Bru, L., Labuhn, I., Pérez-Mejías, C., and Rehfeld, K.: The Potential of Speleothems from Western Europe as Recorders of Regional Climate: A Critical Assessment of the SISAL Database, Quaternary, 1, 30, <https://doi.org/10.3390/quat1030030>, 2018.
- 720 Lechleitner, F. A., Day, C. C., Kost, O., Wilhelm, M., Haghipour, N., Henderson, G. M., and Stoll, H. M.: Stalagmite carbon isotopes suggest deglacial increase in soil respiration in western Europe driven by temperature change, Climate of the Past, 17, 1903–1918, <https://doi.org/10.5194/cp-17-1903-2021>, 2021.
- Li, H., Sinha, A., Anquetil André, A., Spötl, C., Vonhof, H. B., Meunier, A., Kathayat, G., Duan, P., Voarintsoa, N. R. G., Ning, Y., Biswas, J., Hu, P., Li, X., Sha, L., Zhao, J., Edwards, R. L., and Cheng, H.: A multimillennial climatic context for the megafaunal extinctions in Madagascar and Mascarene Islands, Sci. Adv., 6, eabb2459, <https://doi.org/10.1126/sciadv.eabb2459>, 2020.
- 725 Li, H., Spötl, C., and Cheng, H.: A high-resolution speleothem proxy record of the Late Glacial in the European Alps: extending the NALPS19 record until the beginning of the Holocene, Journal of Quaternary Science, 36, 29–39, <https://doi.org/10.1002/jqs.3255>, 2021a.
- 730 Li, H.-C., Ku, T.-L., You, C.-F., Cheng, H., Edwards, R. L., Ma, Z.-B., Tsai, W., and Li, M.-D.: $87\text{Sr}/86\text{Sr}$ and Sr/Ca in speleothems for paleoclimate reconstruction in Central China between 70 and 280 kyr ago, Geochimica et Cosmochimica Acta, 69, 3933–3947, <https://doi.org/10.1016/j.gca.2005.01.009>, 2005.

Li, T.-Y., Baker, J. L., Wang, T., Zhang, J., Wu, Y., Li, H.-C., Blyakharchuk, T., Yu, T.-L., Shen, C.-C., Cheng, H., Kong, X.-G., Xie, W.-L., and Edwards, R. L.: Early Holocene permafrost retreat in West Siberia amplified by reorganization of westerly wind systems, *Commun Earth Environ.*, 2, 1–11, <https://doi.org/10.1038/s43247-021-00238-z>, 2021b.

Liu, D., Wang, Y., Cheng, H., Edwards, R. L., Kong, X., Chen, S., and Liu, S.: Contrasting Patterns in Abrupt Asian Summer Monsoon Changes in the Last Glacial Period and the Holocene, *Paleoceanography and Paleoclimatology*, 33, 214–226, <https://doi.org/10.1002/2017PA003294>, 2018.

Liu, D., Mi, X., Liu, S., and Wang, Y.: Multi-phased Asian hydroclimate variability during Heinrich Stadial 5, *Clim Dyn.*, 60, 4003–4016, <https://doi.org/10.1007/s00382-022-06566-w>, 2023.

Liu, G., Li, X., Chiang, H.-W., Cheng, H., Yuan, S., Chawchai, S., He, S., Lu, Y., Aung, L. T., Maung, P. M., Tun, W. N., Oo, K. M., and Wang, X.: On the glacial-interglacial variability of the Asian monsoon in speleothem $\delta^{18}\text{O}$ records, *Science Advances*, 6, eaay8189, <https://doi.org/10.1126/sciadv.aay8189>, 2020.

Lorrey, A. M., Williams, P. W., Woolley, J.-M., Fauchereau, N. C., Hartland, A., Bostock, H., Eaves, S., Lachniet, M. S., Renwick, J. A., and Varma, V.: Late Quaternary Climate Variability and Change from Aotearoa New Zealand Speleothems: Progress in Age Modelling, Oxygen Isotope Master Record Construction and Proxy-Model Comparisons, *Quaternary*, 3, 24, <https://doi.org/10.3390/quat3030024>, 2020.

Luetscher, M., Moseley, G. E., Festi, D., Hof, F., Edwards, R. L., and Spötl, C.: A Last Interglacial speleothem record from the Sieben Hengste cave system (Switzerland): Implications for alpine paleovegetation, *Quaternary Science Reviews*, 262, 106974, <https://doi.org/10.1016/j.quascirev.2021.106974>, 2021.

Magiera, M., Lechleitner, F. A., Erhardt, A. M., Hartland, A., Kwiecien, O., Cheng, H., Bradbury, H. J., Turchyn, A. V., Riechelmann, S., Edwards, L., and Breitenbach, S. F. M.: Local and Regional Indian Summer Monsoon Precipitation Dynamics During Termination II and the Last Interglacial, *Geophysical Research Letters*, 46, 12454–12463, <https://doi.org/10.1029/2019GL083721>, 2019.

Mangini, A., Spötl, C., and Verdes, P.: Reconstruction of temperature in the Central Alps during the past 2000yr from a $\delta^{18}\text{O}$ stalagmite record, *Earth and Planetary Science Letters*, 235, 741–751, <https://doi.org/10.1016/j.epsl.2005.05.010>, 2005.

Markowska, M., Cuthbert, M. O., Baker, A., Treble, P. C., Andersen, M. S., Adler, L., Griffiths, A., and Frisia, S.: Modern speleothem oxygen isotope hydroclimate records in water-limited SE Australia, *Geochimica et Cosmochimica Acta*, 270, 431–448, <https://doi.org/10.1016/j.gca.2019.12.007>, 2020.

McDonough, L. K., Treble, P. C., Baker, A., Borsato, A., Frisia, S., Nagra, G., Coleborn, K., Gagan, M. K., Zhao, J., and Paterson, D.: Past fires and post-fire impacts reconstructed from a southwest Australian stalagmite, *Geochimica et Cosmochimica Acta*, 325, 258–277, <https://doi.org/10.1016/j.gca.2022.03.020>, 2022.

Meckler, A. N., Clarkson, M. O., Cobb, K. M., Sodemann, H., and Adkins, J. F.: Interglacial Hydroclimate in the Tropical West Pacific Through the Late Pleistocene, *Science*, 336, 1301–1304, <https://doi.org/10.1126/science.1218340>, 2012.

Medina-Elizalde, M., Perritano, S., DeCesare, M., Polanco-Martinez, J., Lases-Hernandez, F., Serrato-Marks, G., and McGee, D.: Southeastern United States Hydroclimate During Holocene Abrupt Climate Events: Evidence From New Stalagmite Isotopic Records From Alabama, *Paleoceanography and Paleoclimatology*, 37, e2021PA004346, <https://doi.org/10.1029/2021PA004346>, 2022.

- 770 Moreno, A., Stoll, H., Jiménez-Sánchez, M., Cacho, I., Valero-Garcés, B., Ito, E., and Edwards, R. L.: A speleothem record of glacial (25–11.6 kyr BP) rapid climatic changes from northern Iberian Peninsula, *Global and Planetary Change*, 71, 218–231, <https://doi.org/10.1016/j.gloplacha.2009.10.002>, 2010.
- 775 Moseley, G. E., Spötl, C., Cheng, H., Boch, R., Min, A., and Edwards, R. L.: Termination-II interstadial/stadial climate change recorded in two stalagmites from the north European Alps, *Quaternary Science Reviews*, 127, 229–239, <https://doi.org/10.1016/j.quascirev.2015.07.012>, 2015.
- 775 Moseley, G. E., Edwards, R. L., Lord, N. S., Spötl, C., and Cheng, H.: Speleothem record of mild and wet mid-Pleistocene climate in northeast Greenland, *Science Advances*, 7, eabe1260, <https://doi.org/10.1126/sciadv.abe1260>, 2021.
- 780 Nagra, G., Treble, P. C., Andersen, M. S., Fairchild, I. J., Coleborn, K., and Baker, A.: A post-wildfire response in cave dripwater chemistry, *Hydrology and Earth System Sciences*, 20, 2745–2758, <https://doi.org/10.5194/hess-20-2745-2016>, 2016.
- 785 Nagra, G., Treble, P. C., Andersen, M. S., Bajo, P., Hellstrom, J., and Baker, A.: Dating stalagmites in mediterranean climates using annual trace element cycles, *Scientific Reports*, 7, 1–12, <https://doi.org/10.1038/s41598-017-00474-4>, 2017.
- Nehme, C., Kluge, T., Verheyden, S., Nader, F., Charalambidou, I., Weissbach, T., Gucel, S., Cheng, H., Edwards, R. L., Satterfield, L., Eiche, E., and Claeys, P.: Speleothem record from Pentadactylos cave (Cyprus): new insights into climatic variations during MIS 6 and MIS 5 in the Eastern Mediterranean, *Quaternary Science Reviews*, 250, 106663, <https://doi.org/10.1016/j.quascirev.2020.106663>, 2020.
- Nehme, C., Verheyden, S., Kluge, T., Nader, F. H., Edwards, R. L., Cheng, H., Eiche, E., and Claeys, P.: Climate variability in the northern Levant from the highly resolved Qadisha record (Lebanon) during the Holocene optimum, *Quaternary Research*, 1–15, <https://doi.org/10.1017/qua.2023.24>, 2023.
- 790 Novello, V. F., Vuille, M., Cruz, F. W., Stríkis, N. M., Paula, M. S. D., Edwards, R. L., Cheng, H., Karmann, I., Jaqueto, P. F., Trindade, R. I. F., Hartmann, G. A., and Moquet, J. S.: Centennial-scale solar forcing of the South American Monsoon System recorded in stalagmites, *Scientific Reports*, 6, <https://doi.org/10.1038/srep24762>, 2016.
- Novello, V. F., Cruz, F. W., Vuille, M., Stríkis, N. M., Edwards, R. L., Cheng, H., Emerick, S., de Paula, M. S., Li, X., Barreto, E. de S., Karmann, I., and Santos, R. V.: A high-resolution history of the South American Monsoon from Last Glacial Maximum to the Holocene, *Sci Rep*, 7, 44267, <https://doi.org/10.1038/srep44267>, 2017.
- 795 Novello, V. F., Cruz, F. W., Moquet, J. S., Vuille, M., de Paula, M. S., Nunes, D., Edwards, R. L., Cheng, H., Karmann, I., Utida, G., Stríkis, N. M., and Campos, J. L. P. S.: Two Millennia of South Atlantic Convergence Zone Variability Reconstructed From Isotopic Proxies, *Geophysical Research Letters*, 45, 5045–5051, <https://doi.org/10.1029/2017GL076838>, 2018.
- 800 Novello, V. F., Cruz, F. W., McGlue, M. M., Wong, C. I., Ward, B. M., Vuille, M., Santos, R. A., Jaqueto, P., Pessenda, L. C. R., Atorre, T., Ribeiro, L. M. A. L., Karmann, I., Barreto, E. S., Cheng, H., Edwards, R. L., Paula, M. S., and Scholz, D.: Vegetation and environmental changes in tropical South America from the last glacial to the Holocene documented by multiple cave sediment proxies, *Earth and Planetary Science Letters*, 524, <https://doi.org/10.1016/j.epsl.2019.115717>, 2019.
- 805 Novello, V. F., William da Cruz, F., Vuille, M., Pereira Silveira Campos, J. L., Stríkis, N. M., Apaéstegui, J., Moquet, J. S., Azevedo, V., Ampuero, A., Utida, G., Wang, X., Paula-Santos, G. M., Jaqueto, P., Ruiz Pessenda, L. C., Breecker, D. O., and Karmann, I.: Investigating $\delta^{13}\text{C}$ values in stalagmites from tropical South America for the last two millennia, *Quaternary Science Reviews*, 255, 106822, <https://doi.org/10.1016/j.quascirev.2021.106822>, 2021.

Oster, J. L., Warken, S. F., Sekhon, N., Arienzo, M. M., and Lachniet, M.: Speleothem Paleoclimatology for the Caribbean, Central America, and North America, *Quaternary*, 2, 5, <https://doi.org/10.3390/quat2010005>, 2019.

810 Oster, J. L., Weisman, I. E., and Sharp, W. D.: Multi-proxy stalagmite records from northern California reveal dynamic patterns of regional hydroclimate over the last glacial cycle, *Quaternary Science Reviews*, 241, 106411, <https://doi.org/10.1016/j.quascirev.2020.106411>, 2020.

Owen, R. A., Day, C. C., Hu, C., Liu, Y., Pointing, M. D., Blättler, C. L., and Henderson, G. M.: Calcium isotopes in caves as a proxy for aridity: Modern calibration and application to the 8.2 kyr event, *Earth and Planetary Science Letters*, 443, 129–138, <https://doi.org/10.1016/j.epsl.2016.03.027>, 2016.

815 Parker, S. E. and Harrison, S. P.: The timing, duration and magnitude of the 8.2 ka event in global speleothem records, *Sci Rep*, 12, 10542, <https://doi.org/10.1038/s41598-022-14684-y>, 2022.

Parker, S. E., Harrison, S. P., Comas-Bru, L., Kaushal, N., LeGrande, A. N., and Werner, M.: A data–model approach to interpreting speleothem oxygen isotope records from monsoon regions, *Climate of the Past*, 17, 1119–1138, <https://doi.org/10.5194/cp-17-1119-2021>, 2021a.

820 Parker, S. E., Harrison, S. P., and Braconnot, P.: Speleothem records of monsoon interannual-interdecadal variability through the Holocene, *Environ. Res. Commun.*, 3, 121002, <https://doi.org/10.1088/2515-7620/ac3eaa>, 2021b.

Pérez-Mejías, C., Moreno, A., Sancho, C., Martín-García, R., Spötl, C., Cacho, I., Cheng, H., and Edwards, R. L.: Orbital-to-millennial scale climate variability during Marine Isotope Stages 5 to 3 in northeast Iberia, *Quaternary Science Reviews*, 224, 105946, <https://doi.org/10.1016/j.quascirev.2019.105946>, 2019.

825 Pérez-Mejías, C., Moreno, A., Bernal-Wormull, J., Cacho, I., Osácar, M. C., Edwards, R. L., and Cheng, H.: Oldest Dryas hydroclimate reorganization in the eastern Iberian Peninsula after the iceberg discharges of Heinrich Event 1, *Quaternary Research*, 101, 67–83, <https://doi.org/10.1017/qua.2020.112>, 2021.

Priestley, S. C., Treble, P. C., Griffiths, A. D., Baker, A., Abram, N. J., and Meredith, K. T.: Caves demonstrate decrease in rainfall recharge of southwest Australian groundwater is unprecedented for the last 800 years, *Commun Earth Environ*, 4, 1–12, <https://doi.org/10.1038/s43247-023-00858-7>, 2023.

Rehfeld, K. and Bühler, J.: Age-depth model ensembles for SISAL v3 speleothem records (2), <https://doi.org/10.5281/zenodo.10570754>, 2024.

830 Riechelmann, D. F. C., Fohlmeister, J., Kluge, T., Jochum, K. P., Richter, D. K., Deininger, M., Friedrich, R., Frank, N., and Scholz, D.: Evaluating the potential of tree-ring methodology for cross-dating of three annually laminated stalagmites from Zoolithencave (SE Germany), *Quaternary Geochronology*, 52, 37–50, <https://doi.org/10.1016/j.quageo.2019.04.001>, 2019.

Riechelmann, D. F. C., Riechelmann, S., Wassenburg, J. A., Fohlmeister, J., Schöne, B. R., Jochum, K. P., Richter, D. K., and Scholz, D.: High-Resolution Proxy Records From Two Simultaneously Grown Stalagmites From Zoolithencave (Southeastern Germany) and their Potential for Palaeoclimate Reconstruction, *Geochem. Geophys. Geosyst.*, 21, <https://doi.org/10.1029/2019GC008755>, 2020.

840 Roberts, M. S., Smart, P. L., and Baker, A.: Annual trace element variations in a Holocene speleothem, *Earth and Planetary Science Letters*, 154, 237–246, [https://doi.org/10.1016/s0012-821x\(97\)00116-7](https://doi.org/10.1016/s0012-821x(97)00116-7), 1998.

Ros, A. and Llamusí, J. L.: Reconstrucción y génesis del karst de Cueva Victoria, Mastia: Revista del Museo Arqueológico Municipal de Cartagena, 111–125, 2012.

- Rowe, P. J., Wickens, L. B., Sahy, D., Marca, A. D., Peckover, E., Noble, S., Özkul, M., Baykara, M. O., Millar, I. L., and Andrews, J. E.: Multi-proxy speleothem record of climate instability during the early last interglacial in southern Turkey, *Palaeogeography, Palaeoclimatology, Palaeoecology*, 538, 109422, <https://doi.org/10.1016/j.palaeo.2019.109422>, 2020.
- Rutledge, H., Baker, A., Marjo, C. E., Andersen, M. S., Graham, P. W., Cuthbert, M. O., Rau, G. C., Roshan, H., Markowska, M., Mariethoz, G., and Jex, C. N.: Dripwater organic matter and trace element geochemistry in a semi-arid karst environment: Implications for speleothem paleoclimatology, *Geochimica et Cosmochimica Acta*, 135, 217–230, <https://doi.org/10.1016/j.gca.2014.03.036>, 2014.
- Scroxton, N., Walczak, M., Markowska, M., Zhao, J., and Fallon, S.: Historical droughts in Southeast Australia recorded in a New South Wales stalagmite, *The Holocene*, 31, 607–617, <https://doi.org/10.1177/0959683620981717>, 2021.
- Serrato Marks, G., Medina-Elizalde, M., Burns, S., Weldeab, S., Lases-Hernandez, F., Cazares, G., and McGee, D.: Evidence for Decreased Precipitation Variability in the Yucatán Peninsula During the Mid-Holocene, *Paleoceanography and Paleoclimatology*, 36, e2021PA004219, <https://doi.org/10.1029/2021PA004219>, 2021.
- Sha, L., Ait Brahim, Y., Wassenburg, J. A., Yin, J., Peros, M., Cruz, F. W., Cai, Y., Li, H., Du, W., Zhang, H., Edwards, R. L., and Cheng, H.: How Far North Did the African Monsoon Fringe Expand During the African Humid Period? Insights From Southwest Moroccan Speleothems, *Geophysical Research Letters*, 46, 14093–14102, <https://doi.org/10.1029/2019GL084879>, 2019.
- Sha, L., Brahim, Y. A., Wassenburg, J. A., Yin, J., Lu, J., Cruz, F. W., Cai, Y., Edwards, R. L., and Cheng, H.: The “Hockey Stick” Imprint in Northwest African Speleothems, *Geophysical Research Letters*, 48, e2021GL094232, <https://doi.org/10.1029/2021GL094232>, 2021.
- Sinha, A., Kathayat, G., Cheng, H., Breitenbach, S. F. M., Berkelhammer, M., Mudelsee, M., Biswas, J., and Edwards, R. L.: Trends and oscillations in the Indian summer monsoon rainfall over the last two millennia, *Nature Communications*, 6, <https://doi.org/10.1038/ncomms7309>, 2015.
- Sinha, A., Kathayat, G., Weiss, H., Li, H., Cheng, H., Reuter, J., Schneider, A. W., Berkelhammer, M., Adali, S. F., Stott, L. D., and Edwards, R. L.: Role of climate in the rise and fall of the Neo-Assyrian Empire, *Science Advances*, 5, eaax6656, <https://doi.org/10.1126/sciadv.aax6656>, 2019.
- Skiba, V.: SISALv3 trace element downsampling code, , <https://doi.org/10.5281/zenodo.8234066>, 2023.
- Skiba, V. and Fohlmeister, J.: Contemporaneously growing speleothems and their value to decipher in-cave processes – A modelling approach, *Geochimica et Cosmochimica Acta*, 348, 381–396, <https://doi.org/10.1016/j.gca.2023.03.016>, 2023.
- Skiba, V., Jouvet, G., Marwan, N., Spötl, C., and Fohlmeister, J.: Speleothem growth and stable carbon isotopes as proxies of the presence and thermodynamical state of glaciers compared to modelled glacier evolution in the Alps, *Quaternary Science Reviews*, 322, 108403, <https://doi.org/10.1016/j.quascirev.2023.108403>, 2023.
- Stoll, H., Mendez-Vicente, A., Gonzalez-Lemos, S., Moreno, A., Cacho, I., Cheng, H., and Edwards, R. L.: Interpretation of orbital scale variability in mid-latitude speleothem d¹⁸O: Significance of growth rate controlled kinetic fractionation effects, *Quaternary Science Reviews*, 127, 215–228, <https://doi.org/10.1016/j.quascirev.2015.08.025>, 2015.
- Stoll, H. M., Cacho, I., Gasson, E., Sliwinski, J., Kost, O., Moreno, A., Iglesias, M., Torner, J., Perez-Mejias, C., Haghipour, N., Cheng, H., and Edwards, R. L.: Rapid northern hemisphere ice sheet melting during the penultimate deglaciation, *Nat Commun*, 13, 3819, <https://doi.org/10.1038/s41467-022-31619-3>, 2022.

Stoll, H. M., Day, C., Lechleitner, F., Kost, O., Endres, L., Sliwinski, J., Pérez-Mejías, C., Cheng, H., and Scholz, D.: Distinguishing the combined vegetation and soil component of $\delta^{13}\text{C}$ variation in speleothem records from subsequent degassing and prior calcite precipitation effects, *Climate of the Past*, 19, 2423–2444, <https://doi.org/10.5194/cp-19-2423-2023>, 2023.

Stríkis, N. M., Cruz, F. W., Barreto, E. A. S., Naughton, F., Vuille, M., Cheng, H., Voelker, A. H. L., Zhang, H., Karmann, I., Edwards, R. L., Auler, A. S., Santos, R. V., and Sales, H. R.: South American monsoon response to iceberg discharge in the North Atlantic, *Proceedings of the National Academy of Sciences*, 115, 3788–3793, <https://doi.org/10.1073/pnas.1717784115>, 2018.

Surić, M., Columbu, A., Lončarić, R., Bajo, P., Bočić, N., Lončar, N., Drysdale, R. N., and Hellstrom, J. C.: Holocene hydroclimate changes in continental Croatia recorded in speleothem $\delta^{13}\text{C}$ and $\delta^{18}\text{O}$ from Nova Grgosova Cave, *The Holocene*, 31, 1401–1416, <https://doi.org/10.1177/09596836211019120>, 2021a.

Surić, M., Bajo, P., Lončarić, R., Lončar, N., Drysdale, R. N., Hellstrom, J. C., and Hua, Q.: Speleothem Records of the Hydroclimate Variability throughout the Last Glacial Cycle from Manita peć Cave (Velebit Mountain, Croatia), *Geosciences*, 11, 347, <https://doi.org/10.3390/geosciences11080347>, 2021b.

Tadros, C. V., Treble, P. C., Baker, A., Fairchild, I., Hankin, S., Roach, R., Markowska, M., and McDonald, J.: ENSO-cave drip water hydrochemical relationship: a 7-year dataset from south-eastern Australia, *Hydrology and Earth System Sciences*, 20, 4625–4640, <https://doi.org/10.5194/hess-20-4625-2016>, 2016.

Tadros, C. V., Markowska, M., Treble, P. C., Baker, A., Frisia, S., Adler, L., and Drysdale, R. N.: Recharge variability in Australia's southeast alpine region derived from cave monitoring and modern stalagmite $\delta^{18}\text{O}$ records, *Quaternary Science Reviews*, 295, 107742, <https://doi.org/10.1016/j.quascirev.2022.107742>, 2022.

Tan, L., Liu, W., Wang, T., Cheng, P., Zang, J., Wang, X., Ma, L., Li, D., Lan, J., Edwards, R. L., Cheng, H., Xu, H., Ai, L., Gao, Y., and Cai, Y.: A multiple-proxy stalagmite record reveals historical deforestation in central Shandong, northern China, *Sci. China Earth Sci.*, 63, 1622–1632, <https://doi.org/10.1007/s11430-019-9649-1>, 2020a.

Tan, L., Li, Y., Wang, X., Cai, Y., Lin, F., Cheng, H., Ma, L., Sinha, A., and Edwards, R. L.: Holocene Monsoon Change and Abrupt Events on the Western Chinese Loess Plateau as Revealed by Accurately Dated Stalagmites, *Geophysical Research Letters*, 47, e2020GL090273, <https://doi.org/10.1029/2020GL090273>, 2020b.

Tan, L., Dong, G., An, Z., Lawrence Edwards, R., Li, H., Li, D., Spengler, R., Cai, Y., Cheng, H., Lan, J., Orozbaev, R., Liu, R., Chen, J., Xu, H., and Chen, F.: Megadrought and cultural exchange along the proto-silk road, *Science Bulletin*, 66, 603–611, <https://doi.org/10.1016/j.scib.2020.10.011>, 2021.

Torner, J., Cacho, I., Moreno, A., Sierro, F. J., Martrat, B., Rodriguez-Lazaro, J., Frigola, J., Arnau, P., Belmonte, Á., Hellstrom, J., Cheng, H., Edwards, R. L., and Stoll, H.: Ocean-atmosphere interconnections from the last interglacial to the early glacial: An integration of marine and cave records in the Iberian region, *Quaternary Science Reviews*, 226, 106037, <https://doi.org/10.1016/j.quascirev.2019.106037>, 2019.

Treble, P., Shelley, J. M. G., and Chappell, J.: Comparison of high resolution sub-annual records of trace elements in a modern (1911–1992) speleothem with instrumental climate data from southwest Australia, *Earth and Planetary Science Letters*, 216, 141–153, [https://doi.org/10.1016/S0012-821X\(03\)00504-1](https://doi.org/10.1016/S0012-821X(03)00504-1), 2003.

Treble, P. C., Baker, A., Abram, N. J., Hellstrom, J. C., Crawford, J., Gagan, M. K., Borsato, A., Griffiths, A. D., Bajo, P., Markowska, M., Priestley, S. C., Hankin, S., and Paterson, D.: Ubiquitous karst hydrological control on speleothem oxygen isotope variability in a global study, *Communications Earth and Environment*, 3, <https://doi.org/10.1038/s43247-022-00347-3>, 2022.

- 920 Tremaine, D. M. and Froelich, P. N.: Speleothem trace element signatures: A hydrologic geochemical study of modern cave dripwaters and farmed calcite, *Geochimica et Cosmochimica Acta*, 121, 522–545, <https://doi.org/10.1016/j.gca.2013.07.026>, 2013.
- Ünal-İmer, E., Shulmeister, J., Zhao, J.-X., Tonguç Uysal, I., Feng, Y.-X., Duc Nguyen, A., and Yüce, G.: An 80 kyr-long continuous speleothem record from Dim Cave, SW Turkey with paleoclimatic implications for the Eastern Mediterranean, *Sci Rep*, 5, 13560, <https://doi.org/10.1038/srep13560>, 2015.
- 925 Ünal-İmer, E., Shulmeister, J., Zhao, J.-X., Uysal, I. T., and Feng, Y.-X.: High-resolution trace element and stable/radiogenic isotope profiles of late Pleistocene to Holocene speleothems from Dim Cave, SW Turkey, *Palaeogeography, Palaeoclimatology, Palaeoecology*, 452, 68–79, <https://doi.org/10.1016/j.palaeo.2016.04.015>, 2016.
- 930 Utida, G., Cruz, F. W., Santos, R. V., Sawakuchi, A. O., Wang, H., Pessenda, L. C. R., Novello, V. F., Vuille, M., Strauss, A. M., Borella, A. C., Stríkis, N. M., Guedes, C. C. F., Dias De Andrade, F. R., Zhang, H., Cheng, H., and Edwards, R. L.: Climate changes in Northeastern Brazil from deglacial to Meghalayan periods and related environmental impacts, *Quaternary Science Reviews*, 250, 106655, <https://doi.org/10.1016/j.quascirev.2020.106655>, 2020.
- 935 Verheyden, S., Keppens, E., Fairchild, I. J., McDermott, F., and Weis, D.: Mg, Sr and Sr isotope geochemistry of a Belgian Holocene speleothem: Implications for paleoclimate reconstructions, *Chemical Geology*, 169, 131–144, [https://doi.org/10.1016/S0009-2541\(00\)00299-0](https://doi.org/10.1016/S0009-2541(00)00299-0), 2000.
- Wainer, K., Genty, D., Blamart, D., Daëron, M., Bar-Matthews, M., Vonhof, H., Dublyansky, Y., Pons-Branchu, E., Thomas, L., van Calsteren, P., Quinif, Y., and Caillon, N.: Speleothem record of the last 180 ka in Villars cave (SW France): Investigation of a large $\delta^{18}\text{O}$ shift between MIS6 and MIS5, *Quaternary Science Reviews*, 30, 130–146, <https://doi.org/10.1016/j.quascirev.2010.07.004>, 2011.
- 940 Waltgenbach, S., Scholz, D., Spötl, C., Riechelmann, D. F. C., Jochum, K. P., Fohlmeister, J., and Schröder-Ritzrau, A.: Climate and structure of the 8.2 ka event reconstructed from three speleothems from Germany, *Global and Planetary Change*, 193, 103266, <https://doi.org/10.1016/j.gloplacha.2020.103266>, 2020.
- 945 Waltgenbach, S., Riechelmann, D. F. C., Spötl, C., Jochum, K. P., Fohlmeister, J., Schröder-Ritzrau, A., and Scholz, D.: Climate Variability in Central Europe during the Last 2500 Years Reconstructed from Four High-Resolution Multi-Proxy Speleothem Records, *Geosciences*, 11, 166, <https://doi.org/10.3390/geosciences11040166>, 2021.
- Wang, Y. J., Cheng, H., Edwards, R. L., An, Z. S., Wu, J. Y., Shen, C. C., and Dorale, J. A.: A high-resolution absolute-dated late Pleistocene Monsoon record from Hulu Cave, China., *Science (New York, N.Y.)*, 294, 2345–2348, <https://doi.org/10.1126/science.1064618>, 2001.
- 950 Ward, B. M., Wong, C. I., Novello, V. F., McGee, D., Santos, R. V., Silva, L. C. R., Cruz, F. W., Wang, X., Edwards, R. L., and Cheng, H.: Reconstruction of Holocene coupling between the South American Monsoon System and local moisture variability from speleothem $\delta^{18}\text{O}$ and $^{87}\text{Sr}/^{86}\text{Sr}$ records, *Quaternary Science Reviews*, 210, 51–63, <https://doi.org/10.1016/j.quascirev.2019.02.019>, 2019.
- 955 Warken, S. F., Fohlmeister, J., Schröder-Ritzrau, A., Constantin, S., Spötl, C., Gerdes, A., Esper, J., Frank, N., Arps, J., Terente, M., Riechelmann, D. F. C., Mangini, A., and Scholz, D.: Reconstruction of late Holocene autumn/winter precipitation variability in SW Romania from a high-resolution speleothem trace element record, *Earth and Planetary Science Letters*, 499, 122–133, <https://doi.org/10.1016/j.epsl.2018.07.027>, 2018.
- Warken, S. F., Vieten, R., Winter, A., Spötl, C., Miller, T. E., Jochum, K. P., Schröder-Ritzrau, A., Mangini, A., and Scholz, D.: Persistent Link Between Caribbean Precipitation and Atlantic Ocean Circulation During the Last Glacial Revealed by a

Speleothem Record From Puerto Rico, Paleoceanography and Paleoclimatology, 35, e2020PA003944,
960 https://doi.org/10.1029/2020PA003944, 2020.

Warken, S. F., Schorndorf, N., Stinnesbeck, W., Hennhoefer, D., Stinnesbeck, S. R., Förstel, J., Steidle, S. D., Avilés Olguín, J., and Frank, N.: Solar forcing of early Holocene droughts on the Yucatán peninsula, *Sci Rep*, 11, 13885, https://doi.org/10.1038/s41598-021-93417-z, 2021.

965 Wassenburg, J. A., Scholz, D., Jochum, K. P., Cheng, H., Oster, J., Immenhauser, A., Richter, D. K., Häger, T., Jamieson, R. A., Baldini, J. U. L., Hoffmann, D., and Breitenbach, S. F. M.: Determination of aragonite trace element distribution coefficients from speleothem calcite–aragonite transitions, *Geochimica et Cosmochimica Acta*, 190, 347–367, https://doi.org/10.1016/j.gca.2016.06.036, 2016.

970 Wassenburg, J. A., Vonhof, H. B., Cheng, H., Martínez-García, A., Ebner, P.-R., Li, X., Zhang, H., Sha, L., Tian, Y., Edwards, R. L., Fiebig, J., and Haug, G. H.: Penultimate deglaciation Asian monsoon response to North Atlantic circulation collapse, *Nat. Geosci.*, 14, 937–941, https://doi.org/10.1038/s41561-021-00851-9, 2021.

Weber, M., Scholz, D., Schröder-Ritzrau, A., Deininger, M., Spötl, C., Lugli, F., Mertz-Kraus, R., Jochum, K. P., Fohlmeister, J., Stumpf, C. F., and Riechelmann, D. F. C.: Evidence of warm and humid interstadials in central Europe during early MIS 3 revealed by a multi-proxy speleothem record, *Quaternary Science Reviews*, 200, 276–286, https://doi.org/10.1016/j.quascirev.2018.09.045, 2018.

975 Weber, M., Hinz, Y., Schöne, B. R., Jochum, K. P., Hoffmann, D., Spötl, C., Riechelmann, D. F. C., and Scholz, D.: Opposite Trends in Holocene Speleothem Proxy Records From Two Neighboring Caves in Germany: A Multi-Proxy Evaluation, *Frontiers in Earth Science*, 9, 2021.

980 Welte, C., Fohlmeister, J., Wertnik, M., Wacker, L., Hattendorf, B., Eglinton, T. I., and Spötl, C.: Climatic variations during the Holocene inferred from radiocarbon and stable carbon isotopes in speleothems from a high-alpine cave, *Clim. Past*, 17, 2165–2177, https://doi.org/10.5194/cp-17-2165-2021, 2021.

Wendt, K. A., Häuselmann, A. D., Fleitmann, D., Berry, A. E., Wang, X., Auler, A. S., Cheng, H., and Edwards, R. L.: Three-phased Heinrich Stadial 4 recorded in NE Brazil stalagmites, *Earth and Planetary Science Letters*, 510, 94–102, https://doi.org/10.1016/j.epsl.2018.12.025, 2019.

985 Wendt, K. A., Li, X., Edwards, R. L., Cheng, H., and Spötl, C.: Precise timing of MIS 7 substages from the Austrian Alps, *Climate of the Past*, 17, 1443–1454, https://doi.org/10.5194/cp-17-1443-2021, 2021.

Wilcox, P. S., Honiat, C., Trüssel, M., Edwards, R. L., and Spötl, C.: Exceptional warmth and climate instability occurred in the European Alps during the Last Interglacial period, *Commun Earth Environ*, 1, 1–6, https://doi.org/10.1038/s43247-020-00063-w, 2020.

990 Winter, A., Zanchettin, D., Lachniet, M., Vieten, R., Pausata, F. S. R., Ljungqvist, F. C., Cheng, H., Edwards, R. L., Miller, T., Rubinetti, S., Rubino, A., and Taricco, C.: Initiation of a stable convective hydroclimatic regime in Central America circa 9000 years BP, *Nat Commun*, 11, 716, https://doi.org/10.1038/s41467-020-14490-y, 2020.

995 Wolf, A., Baker, J. L., Tjallingii, R., Cai, Y., Osinzev, A., Antonosyan, M., Amano, N., Johnson, K. R., Skiba, V., McCormack, J., Kwiecien, O., Chervyatsova, O. Y., Dublyansky, Y. V., Dbar, R. S., Cheng, H., and Breitenbach, S. F. M.: Western Caucasus regional hydroclimate controlled by cold-season temperature variability since the Last Glacial Maximum, *Commun Earth Environ*, 5, 1–10, https://doi.org/10.1038/s43247-023-01151-3, 2024.

Wong, C. I. and Breecker, D. O.: Advancements in the use of speleothems as climate archives, *Quaternary Science Reviews*, 127, 1–18, <https://doi.org/10.1016/j.quascirev.2015.07.019>, 2015.

Wortham, B. E., Wong, C. I., Silva, L. C. R., McGee, D., Montañez, I. P., Troy Rasbury, E., Cooper, K. M., Sharp, W. D., Glessner, J. J. G., and Santos, R. V.: Assessing response of local moisture conditions in central Brazil to variability in regional monsoon intensity using speleothem $^{87}\text{Sr}/^{86}\text{Sr}$ values, *Earth and Planetary Science Letters*, 463, 310–322, <https://doi.org/10.1016/j.epsl.2017.01.034>, 2017.

Wright, K. T., Johnson, K. R., Bhattacharya, T., Marks, G. S., McGee, D., Elsbury, D., Peings, Y., Lacaille-Muzquiz, J., Lum, G., Beramendi-Orosco, L., and Magnusdottir, G.: Precipitation in Northeast Mexico Primarily Controlled by the Relative Warming of Atlantic SSTs, *Geophysical Research Letters*, 49, <https://doi.org/10.1029/2022GL098186>, 2022.

Wu, Y., Li, T.-Y., Yu, T.-L., Shen, C.-C., Chen, C.-J., Zhang, J., Li, J.-Y., Wang, T., Huang, R., and Xiao, S.-Y.: Variation of the Asian summer monsoon since the last glacial-interglacial recorded in a stalagmite from southwest China, *Quaternary Science Reviews*, 234, 106261, <https://doi.org/10.1016/j.quascirev.2020.106261>, 2020.

Yang, X., Yang, H., Wang, B., Huang, L.-J., Shen, C.-C., Edwards, R. L., and Cheng, H.: Early-Holocene monsoon instability and climatic optimum recorded by Chinese stalagmites, *The Holocene*, 29, 1059–1067, <https://doi.org/10.1177/0959683619831433>, 2019.

Zhang, H., Ait Brahim, Y., Li, H., Zhao, J., Kathayat, G., Tian, Y., Baker, J., Wang, J., Zhang, F., Ning, Y., Edwards, R. L., and Cheng, H.: The Asian Summer Monsoon: Teleconnections and Forcing Mechanisms—A Review from Chinese Speleothem $\delta^{18}\text{O}$ Records, *Quaternary*, 2, 26, <https://doi.org/10.3390/quat2030026>, 2019.

Zhang, H., Zhang, X., Cai, Y., Sinha, A., Spötl, C., Baker, J., Kathayat, G., Liu, Z., Tian, Y., Lu, J., Wang, Z., Zhao, J., Jia, X., Du, W., Ning, Y., An, Z., Edwards, R. L., and Cheng, H.: A data-model comparison pinpoints Holocene spatiotemporal pattern of East Asian summer monsoon, *Quaternary Science Reviews*, 261, 106911, <https://doi.org/10.1016/j.quascirev.2021.106911>, 2021a.

Zhang, H., Cheng, H., Sinha, A., Spötl, C., Cai, Y., Liu, B., Kathayat, G., Li, H., Tian, Y., Li, Y., Zhao, J., Sha, L., Lu, J., Meng, B., Niu, X., Dong, X., Liang, Z., Zong, B., Ning, Y., Lan, J., and Edwards, R. L.: Collapse of the Liangzhu and other Neolithic cultures in the lower Yangtze region in response to climate change, *Science Advances*, 7, eabi9275, <https://doi.org/10.1126/sciadv.abi9275>, 2021b.

Zhang, H., Cheng, H., Spötl, C., Zhang, X., Cruz, F. W., Sinha, A., Auler, A. S., Stríkis, N. M., Wang, X., Kathayat, G., Li, X., Li, H., Pérez-Mejías, C., Cai, Y., Ning, Y., and Edwards, R. L.: Gradual South-North Climate Transition in the Atlantic Realm Within the Younger Dryas, *Geophysical Research Letters*, 48, e2021GL092620, <https://doi.org/10.1029/2021GL092620>, 2021c.

Zhao, J., Cheng, H., Yang, Y., Liu, W., Zhang, H., Li, X., Li, H., Ait-Brahim, Y., Pérez-Mejías, C., and Qu, X.: Role of the Summer Monsoon Variability in the Collapse of the Ming Dynasty: Evidences From Speleothem Records, *Geophysical Research Letters*, 48, e2021GL093071, <https://doi.org/10.1029/2021GL093071>, 2021.

Zhao, K., Wang, Y., Edwards, R. L., Cheng, H., Kong, X., Liu, D., Shao, Q., Cui, Y., Huang, C., Ning, Y., and Yang, X.: Late Holocene monsoon precipitation changes in southern China and their linkage to Northern Hemisphere temperature, *Quaternary Science Reviews*, 232, 106191, <https://doi.org/10.1016/j.quascirev.2020.106191>, 2020.